이학박사학위 논문

글루코코르티코이드와 일주기시계 유전자의 분자적 상호작용

Molecular interaction between glucocorticoid and circadian clock genes

2014년 2월

서울대학교 대학원

뇌과학협동과정

천솔미

글루코코르티코이드와 일주기시계 유전자의 분자적 상호작용

Molecular interaction between glucocorticoid and circadian clock genes

지도교수 김경진

이 논문을 이학박사 학위논문으로 제출함
2013년 12월

서울대학교 대학원
뇌과학협동과정
천솔미

천솔미의 이학박사 학위논문을 인준함
2013년 12월

위 원 장 최 성 우

부위원장 김 경 진

위 원 정 진 하

위 원 이 건 수

위 원 선 웅

Molecular interaction between glucocorticoid and circadian clock genes

A dissertation submitted in partial fulfillment of the requirement for the degree of

DOCTOR OF PHILOSOPHY

To the Faculty of the

Interdisciplinary Program in Neuroscience

at

Seoul National University

by

Solmi Cheon

Date Approved:

Dec 18, 2013

Sukwoo Choi

Chul Hoon Chung

Woong Sun

ABSTRACT

Molecular interaction between glucocorticoid and circadian clock genes

Solmi Cheon
Interdisciplinary Program in Neuroscience
The Graduate School
Seoul National University

The circadian clock is an internal timekeeping system that regulates physiology, metabolism and behavior with about 24-hr period. In mammals, it has hierarchical structure: the master clock in the brain regulates the peripheral clocks. The master clock, which is located in the suprachiasmatic nucleus of the hypothalamus, synchronizes peripheral clocks through neural and humoral factors. Among many synchronizing signals, an attractive one is glucocorticoid (GC) hormone, of which the plasma level exhibits the circadian pattern. The hormone can entrain most of peripheral tissues without the interference of the master clock, because the GC receptor (GR) is ubiquitously expressed in peripheral tissues, not in the master clock.

GC directly regulates circadian clock genes, including Period1 (Per1)

and Period2 (Per2). The previous study revealed that there is a functional glucocorticoid response element (GRE) in Per1 promoter, however, the GRE had not been found in Per2 promoter. Therefore, I attempted to explore the molecular mechanism of GC-mediated Per2 expression. I observed that GC induced a prominent Per2 induction and delayed circadian phase compared to other synchronizing signals. Using the promoter prediction tool, I found that the GRE in the highly conserved region of Per2 promoter. The GRE was overlapped with E-box by 1-bp. Interestingly, the mutation of E-box inhibited GC responsiveness of Per2, which was also abolished in *Bmal1*$^{-/-}$ MEFs. The involvement of Bmal1 in GC responsiveness might be a special regulatory mechanism because other GRE-containing genes, such as Per1 and mouse mammary tumor virus (MMTV) still exhibited GC responsiveness in *Bmal1*$^{-/-}$ MEFs. The chromatin immunoprecipitation assay using the GR antibody showed that Bmal1 was required for the binding of GR to the GRE of Per2 promoter. To identify the functional importance of GC-mediated Per2 induction, I generated the adenovirus that expresses the fusion protein of PER2 and LUCIFERASE under Per2 promoter. When *Per2*$^{-/-}$ MEFs were transduced with either GRE or E-box mutant adenovirus, GC-mediated Per2 induction was decreased and the circadian phase was advanced. Taken together, this study reveals that Bmal1-dependent Per2 induction by GC signaling rendered the circadian phase delay.

Based on a novel GC regulation mechanism, which requires Bmal1, I investigated global regulatory patterns of Bmal1 on GC-responsive genes to discover other Bmal1-modulated GC-responsive genes. I performed the microarray experiment using WT and *Bmal1*$^{-/-}$ MEFs after the treatment of vehicle or dexamethasone and analyzed the data by 2-way ANOVA. More than half of GC-responsive genes exhibited altered GC responsiveness in *Bmal1*$^{-/-}$ MEFs. To explore the biological meaning of this regulation mechanism, I analyzed the enrichment of gene ontology terms with the bioinformatics tool to find out Bmal1-modulated GC-responsive genes. Interestingly, Bmal1-modulated GC-responsive genes were highly related to the terms, glycoprotein, oxidation-reduction and response to stimulus, while non-Bmal1-modulated GC-responsive genes were highly related to the terms, intracellular, protein binding and intracellular signal transduction. Then, results suggest that Bmal1 is widely involved in GC-regulation mechanism and Bmal1-modulated GC-responsive genes are involved in some biological processes, including glycosylation, oxidation-reduction and the response to stimulus. These finding may contribute to future understanding for GC action mechanisms and the interaction between GC and circadian clock genes.

Keywords: circadian rhythm, glucocorticoid, Period2, Bmal1, microarray

Student number**:** 2006-22971

CONTENTS

CHAPTER 2. The global regulatory feature of Bmal1 on glucocorticoid-responsive genes

LIST OF FIGURES

Page

BACKGROUND AND PURPOSE

BACKGROUND

1. Circadian clock

1.1 What is circadian clock?

Most of living organisms on the earth possess the internal clock to anticipate the daily environmental change, which is called the circadian clock. The term “Circadian” comes from the Latin: “circa” means around and “diem” means a day. The circadian clock makes physiology and behavior to have about 24-hr period, including sleep/wake cycle, metabolism in humans and photosynthesis in plants and even in cyanobacteria. The basic concept of this clock is that the rhythm is generated from endogenous factors, not from any external ones. For example, nocturnal mice move around in the night and when the light turns off, they maintain their activity at the expected night time. Another feature of the circadian clock is temperature compensation. While most of biological activities rely on the temperature, the period of the circadian rhythm is almost same over a broad range of physiological temperatures (Vitaterna et al., 2001).

1.2 Molecular feedback loops of circadian clock

After discovering Period gene of Drosophila in 1971, circadian clock genes were sequentially reported from 1990s (Turek and Kolker, 2001). At

present, it has been known that two molecular feedback loops constitute the driving force for the circadian rhythm. The center of the feedback loops is two transcription factors, which are Circadian Locomotor Output Cycles Kaput (CLOCK) and brain and muscle ARNT-like protein 1 (BMAL1). CLOCK:BMAL1 heterodimer binds to the E-box of clock-controlled genes such as Period (Per) 1-3, Cryptochrome (Cry) 1-2, Rev-erbα and RAR-related orphan receptor α (RORα). As the protein levels of Pers and Crys are increased, they translocate into the nucleus to repress the transcriptional activity of CLOCK:BMAL1. Therefore, the expression levels of Pers and Crys return to the basal level. This negative feedback loop is necessary for generation of circadian rhythm and, thereby, called for the core loop. The second feedback loop regulates the oscillation of Bmal1 expression. Two clock-controlled genes, Rev-erb α and RORα, bind to Rev-erb/ROR binding element (RRE) of Bmal1 promoter to repress or activate Bmal1 transcription. This feedback loop is called the stabilizing loop because it is thought to stabilize circadian oscillations (Figure 1) (Gallego and Virshup, 2007).

1.3 Hierarchical organization of circadian clock system

In mammals, the master clock is located in the suprachiasmatic nucleus (SCN) of the anterior hypothalamus. The SCN is composed of ~20,000 neurons, each of which is an autonomous circadian oscillator. The coherent

Figure 1. Molecular bases of circadian rhythm

Two transcription factors, CLOCK and BMAL1, bind to E-box on the promoter of clock-controlled genes, including Pers, Crys, Rev-erbα and Rorα. Translated PER and CRY proteins are post-translationally modified, accumulate in the cytoplasm and, then, translocate to the nucleus to repress CLOCK:BMAL1 transcriptional activity. On the other hand, Rev-erbα and Rorα regulates Bmal1 expression through the binding of RRE in Bmal1 promoter.

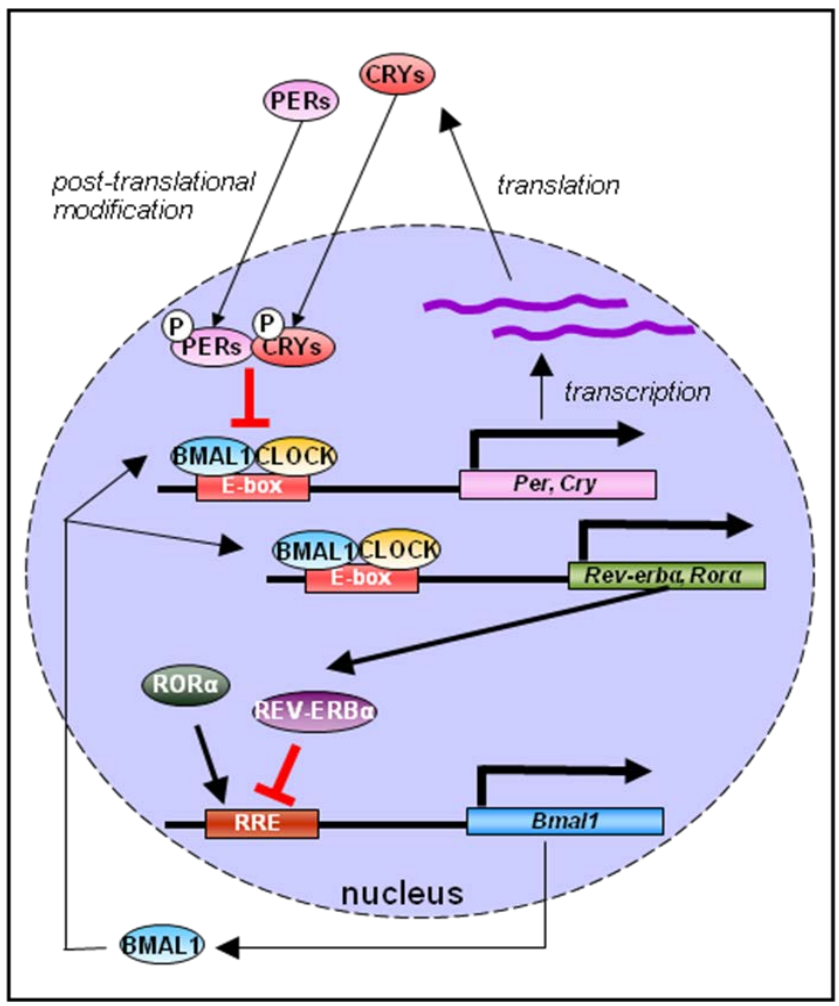
PERs
CRYs
post-translational
modification
translation
P
PERs
P
CRYs
transcription
BMAL1
CLOCK
E-box
Per, Cry
BMAL1
CLOCK
E-box
Rev-erbα, Rorα
RORα
REV-ERBα
RRE
Bmal1
nucleus
BMAL1

neuronal activities in the SCN generate strong circadian rhythm with about 24-hr period (Mohawk et al., 2012). As the endogenous rhythm of the SCN is not exactly matched to the light/dark cycle, it should be corrected by the environmental resetting signals, such as the light. When the light reaches the eye, the signal is transmitted *via* the retino-hypothalamic tract (RHT) into the SCN (Stratmann and Schibler, 2006; Vitaterna et al., 2001).

Circadian rhythm exists not only in the SCN, but in peripheral cells. When peripheral tissues or cells were incubated in culture media, they still maintained the circadian oscillation. Therefore, to make overt rhythm of physiology and behavior, the rhythms of the SCN and peripheral tissues have to be synchronized. Several cues including neuronal system, humoral factors and temperature are known for synchronizing signals between the SCN and peripheral tissues (Mohawk et al., 2012).

1.4 Resetting circadian rhythm in the SCN

Circadian period of each SCN neuron varies from 22-hr to 30-hr, but the intercellular coupling organizes into the overall rhythms with about 24-hr period. It seems that this heterogeneous population generates two types of advantages: phase lability and phase plasticity. The SCN waveform exhibits narrow and high amplitude in short photoperiod, while it shows broad and low amplitude in long photoperiod. When the light signal reaches the SCN, it resets the circadian rhythm differently according to the circadian time.

Almost all species exhibit phase-dependent responses to the light, of which graphical display is called a phase-response curve. Light at the early subjective night induces a phase delay and light at the late subjective night induces a phase advance (Mohawk et al., 2012; Vitaterna et al., 2001).

Light at the subjective night stimulates the secretion of glutamate and pituitary adenylate cyclase-activating protein (PACAP) from the RHT. Then, it induces several signaling pathways that are related to the chromatin remodeling and the induction of immediate early genes and clock genes in the SCN. Because a small subset of SCN neurons receives the signal from the RHT, neighboring neurons are synchronized by the gap junction and several neuropeptides, such as vasoactive intestinal polypeptide (VIP), arginine vasopressin (AVP), γ-aminobutyric acid (GABA), ghrelin-releasing peptide (GRP) (Albrecht, 2012).

1.5 Synchronization between the SCN and peripheral clocks

Peripheral clocks are synchronized by several factors, including the autonomic nervous system, body temperature, humoral factors and feeding/fasting cycles (Albrecht, 2012). The sympathetic pathway from the SCN regulates circadian oscillations of plasma glucose, the sensitivity of the adrenal gland to the adrenocorticotropic hormone (Cailotto et al, 2005; Kalsbeek et al, 2004; Kalsbeek et al, 2010). Although many humoral signals are considered to be synchronizing signals, glucocorticoid (GC) is

regarded as a strong one from several reasons. The level of GC oscillates in a circadian fashion and it reaches almost all of the body, except the SCN. In addition, Dexamethasone (DEX), which is a synthetic GC, can initiate and shift the circadian rhythm of peripheral tissues and cultured fibroblasts (Balsalobre et al., 2000a). Body temperature, of which the circadian fluctuation is driven by the SCN, can reset the circadian rhythm of peripheral clocks, including liver, kidney, lung and fibroblasts (Abraham et al, 2010; Brown et al, 2002; Buhr et al, 2010; Kormmann et al, 2007). Irrespective of the SCN, food and food-related signals are able to produce circadian patterns (Hara et al 2001; Pezuk et al 2010). The change of feeding schedule can uncouple the phase relationship between the master clock and peripheral clocks, suggesting that changes in metabolism may influence the circadian clock system (Albrecht, 2012)

2. Physiological roles of circadian clock

2.1 Mutual relationship between metabolism and circadian clock

The role of circadian clock for metabolic homeostasis has revealed from several circadian clock gene mutant mice. *Bmal1*$^{-/-}$ mice exhibited abolished oscillation of plasma glucose and triglycerides and pancreas-specific knockout mice got *diabetes mellitus*. *Clock*$^{-/-}$ mice showed reduced arterial blood pressure, altered renal function and excretion of diluted urine. *Per1*^{Brdm1} mice showed increased urinary sodium excretion and *Per2*^{Brdm1}

mice exhibited altered lipid metabolism and lower body weight. *Cry1*$^{-/-}$*Cry2*$^{-/-}$ mice had hyperglycemia and salt-sensitive hypertension. Moreover, components in the stabilizing loop also affect on metabolic parameters. *Rev-erbα*$^{-/-}$ mice had increased serum triglycerides and *Rorα*$^{-/-}$ mice showed reduced plasma triglycerides and high density lipoprotein (Sahar and Sassone-Corsi, 2012).

Circadian clock regulates metabolism through controlling multiple steps of various metabolic pathways. One method is to control the expression or the enzymatic activity of rate-limiting enzymes. For example, the activity of 3-hydroxy-3-methyl-glutaryl-CoA reductase (HMG-CoA reductase), which is the rate-limiting enzyme in cholesterol biosynthesis, is highest at night and the expression of nicotinamide phosphoribosyltransferase (NAMPT), which is the rate-limiting enzyme in NAD+ salvage pathway, shows circadian rhythmicity. The expression of aminolevulinate synthase 1 (ALAS1), which is the rate-limiting enzyme in heme biosynthesis, also oscillates in a circadian fashion. Another method is to regulate the expression and the activity of nuclear receptors because they regulate many biological processes, including growth, development, reproduction and metabolism. It has been reported that the expression of several nuclear receptors such as Rev-erbα, Rorα and peroxisome proliferator-activated receptor α (PPARα) was controlled by CLOCK:BMAL1. Furthermore, the microarray analysis revealed that the expression of 25 nuclear receptors exhibited circadian

patterns in a tissue-specific manner. On the other hand, PER proteins interact with several nuclear receptors. As PER protein expressions show the circadian rhythm, the interaction between PER and nuclear receptors can induce the activity of nuclear receptors in a circadian manner. with the interaction partners of PER2 are PPARα, ERα, REV-ERBα, HNF4α, TRα, NURR1, RORα and PPARγ (Schmutz et al., 2010). Per2 gene is also related to the glucose homeostasis (So et al., 2009). Indirectly, the circadian clock machinery perceives the energy level through nutrient sensors, such as sirtuin 1 (sirt1) and AMP-activated kinase (AMPK). The activity of SIRT1, which is a NAD^+-dependent deacetylase, reflects the energy status in the cell because its activity is regulated by NAD^+/NADH ratio. It was observed that SIRT1 activity oscillated in a circadian fashion and SIRT1 regulated circadian rhythms by deacetylating histon H3 Lys9 and Lys14, BMAL1 and PER2. When AMP level rises, the activated AMPK turns on the catabolic processes. The activity of AMPK is rhythmic in the mouse liver, hypothalamus and fibroblasts. AMPK modulates the circadian clock by phosphorylation of CRY1, which leads to the rapid degradation through the recruitment of F-box and leucine-rich-repeat protein 3 (FBXL3). It also activates casein kinase 1ε (CK1ε) and, thereby, leads to the degradation of PER2 (Sahar and Sassone-Corsi, 2012).

2.2 Circadian disturbance and metabolic syndrome

Although circadian clock is able to be entrained by the environmental time cue, frequent or abrupt change of the environment brings about trouble in physiology. For example, shift workers experience the frequent entrainment process against their will. Epidemiological studies showed that many shift workers suffered from the metabolic syndrome, suggesting that the metabolism and circadian rhythm are closely associated (De Bacquer et al., 2009; Esquirol et al., 2009). Furthermore, high-density lipoproteins were decreased and circulating triglycerides were increased in nighttime shift workers, who were also prone to the obesity (Bellet and Sassone-Corsi, 2010). When, behavioral and circadian cycles were desynchronized it caused a decrease in leptin and an increase in glucose and insulin levels (Scheer et al., 2009). Moreover, exposure to light at night disturbed the timing of food intake, reduced glucose tolerance and led to weight gain in mice (Fonken et al., 2010). Jet lag also induces the de-synchronization of circadian rhythms between the SCN and the peripheral tissues. The symptoms of jet lag includes sleep disturbance during the night, daytime sleepiness, decrease cognitive ability, malaise, indigestion, frequent urination, the irritation of eye and nose, muscle cramps, headache, nausea. Frequent experience of the travel across time zones often induce chronic sleep disturbances, malaise, irritability, and performance impairment like shift workers (Cho et al., 2000). As the symptoms of jet lag may be big problems for some people, including pilots and individuals that requires the

concentration, A possible drug target for jet lag is GC hormone, because it affects the time to adapt to new environment in models of daytime restricted feeding or 6-hr phase-shift of LD cycle (Kiessling et al., 2010; Le Minh et al., 2001).

2.3 Genetics of human circadian disorders

Circadian rhythm in humans can be non-invasively examined by the observation of sleep wake/cycle, which is controlled by homeostatic process and circadian process. It seems that a circadian process decides the threshold of wakefulness. Actually, several human sleep disorders are related to the dysfunction of circadian rhythm. Patients with familial advanced sleep phase syndrome (FASPS), who fall asleep and awake 3-4 hr earlier than normal people. They didn't perceive the inconvenience of the syndrome, but become aware it after the forced sleep/wake cycle. The syndrome is derived from S662G mutation of PER2, which blocks the phosphorylation and results in the phase advance through the regulation of the protein stability or nuclear retention of PER2 (Toh et al., 2001; Vanselow et al., 2006). In humans, delayed sleep phase syndrome (DSPS) is the most common type of circadian rhythm sleep disorder. Sleep/wake cycle of DSPS patients is delayed by 2 or more hours. T3111C polymorphism in the 3′UTR of CLOCK, which is related to the diurnal preference, was suggested as a reason for DSPS, but there are pros and cons (Katzenberg et al.,

1998; Mishima et al., 2005; Robilliard et al., 2002). Another study reported that S408N of CSNK1E prevented the onset of DSPS and non-24-hour sleep-wake syndrome (Takano et al., 2004). The other study reported that C111G polymorphism in the 5′-UTR of PER2 might be related to the morning preference (Carpen et al., 2005). Although Per3 has no precise role in mouse circadian rhythm, it is associated with the sleep phase in the human. Variable-number tandem-repeat (vNTR) polymorphism in the PER3 gene is related to DSPS, however, the association of polymorphism repeat number with DSPS may be different according to the latitude (Takahashi et al., 2008).

3. Glucocorticoid

3.1 Glucocorticoid hormone

GC is a steroid hormone that is released from the cortex of the adrenal gland. The name is a compound word (glucose + cortex) that comes from its role for the regulation of the metabolism of glucose and its synthesis in the adrenal cortex. The major GC is cortisol in human and corticosterone in mouse. The hormone has diverse effects, including metabolism, immune response, development, arousal, cognition and body fluid homeostasis. The hormone level is regulated by the negative feedback mechanism of the hypothalamic-pituitary-adrenal gland (HPA) axis. When the organism meets stimulus such as stress or physical activity, corticotrophin-releasing

hormone (CRH) is released from the paraventricular nucleus (PVN) of the hypothalamus. CRH stimulates the release of the adrenocorticotropic hormone (ACTH) in the anterior lobe of the pituitary gland. Then, ACTH reaches to the adrenal gland through the blood, leading to the secretion of GC in the cortex of the adrenal gland. If GC level is highly elevated, it suppresses the release of CRH.

3.2 Molecular mechanisms of GC action

GC exerts its action through the genomic or non-genomic fashion. In the genomic action mechanism, it is bound to the glucocorticoids receptor (GR) in the cytoplasm. When the GR does not meet GC, it is surrounded by heat shock proteins and other proteins such as immunophilins and calreticulin. The ligand binding domain of GR recognizes GC, then, GR is dissociated from the multi-protein complex and translocates to the nucleus. In the nucleus it acts as a transactivator or a transrepressor according to the promoter context. The representative mechanism for the transactivation is that GR homodimer directly binds to the glucocorticoids response element (GRE). However, there are other types of regulation mechanisms for the transactivation because of the interaction between GR and other transcription factors. GRE-bound GR can interact with other transcription factors in the composite GRE that is consisted of GRE and other transcription factor binding site. It can also regulate the transcriptional

activity through tethering, not direct binding to DNA. In a similar fashion, it is able to regulate transrepression mechanisms. The sequence of negative GRE (nGRE) is different from GRE, but GR homodimer binds to the sequence and turns off the transcription. It can also repress transcriptional activities through the composite GRE and the tethering mechanism. In addition, the competition with other transcription factor for DNA binding and transcriptional squelching is able to repress the transcriptional activity (Figure 2).

3.3 The interaction between GC and the circadian clock

As referred to earlier, GC level fluctuate in a circadian fashion. It may be related to the timing of the activity onset, because the peak time is around dawn in the diurnal animal, such as humans and is around dusk in the nocturnal animal, such as mice. The GC rhythm is thought to be regulated by two mechanisms. The relay of the time information from the SCN to the PVN results in the activation of the HPA axis, which induces the circadian oscillation pattern of ACTH and GC (Dickmeis, 2009; Lightman and Conway-Campbell, 2010). Neural connection from the SCN to the adrenal gland also delivers the resetting signal from the light pulse. The light exposure is able to induce GC release from the adrenal grand only when the SCN is intact (Ishida et al., 2005; Niijima et al., 1992). Circadian control of GC level is evident from several reports. *Per1*^{Brdm1} mice had

Figure 2. Molecular mechanisms of GC action

GC exerts genomic actions through various regulation mechanisms. Depending on the promoter context, it turns on or off the transcription. GC-bound GR directly binds to the GRE, resulting in the transcriptional activation. Other types of regulation mechanisms are described in the text.

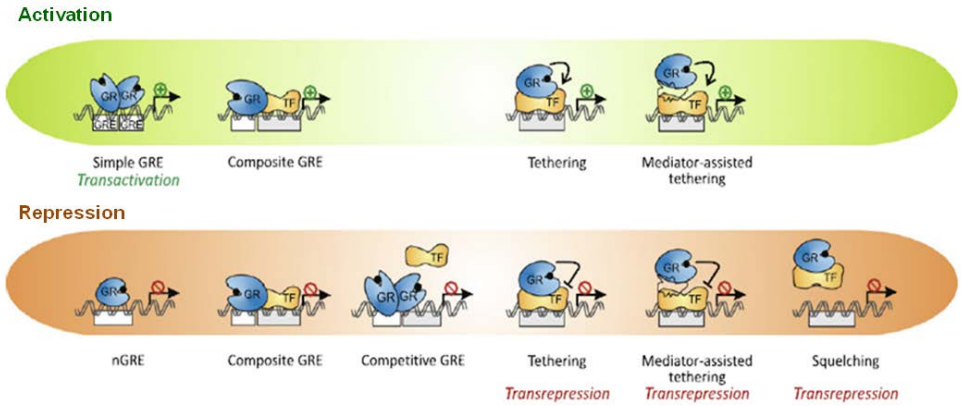

<Modified from Ratman *et al.*, 2012, *Mol Cell Endocrinol*>

markedly elevated fecal GC levels without the circadian fluctuation and *Per2*^{Brdm1} mice had elevated but fluctuating fecal GC levels (Dallmann et al., 2006). In the other report, *Per2*$^{-/-}$ mice lost circadian patterns of plasma GC (Yang et al., 2009). Moreover, the local clock in the adrenal gland contributes to GC rhythm to some extent. The adrenal-specific ablation of steroidogenic acute regulatory gene dampened GC rhythm only after the long duration of constant darkness condition (Son et al., 2008).

Reciprocally, it has been well known that GC influences on the circadian system. The effects of GC on several circadian clock genes were identified. When mice were subjected to restraint stress, elevated GC levels increased Per1 expression level through a GRE in Per1 promoter (Yamamoto et al., 2005a). From the chromatin immunoprecipitation-sequencing (ChIP-seq) analysis, So et al. found the intronic GRE of Per2 gene (So et al., 2009). Unlike Per1 and Per2, GC represses Rev-erbα expression, although the molecular mechanism remains unexplored (Torra et al., 2000). The contribution of GC to the entrainment process is evident, in that the adrenalectomy and liver-specific knockout of GR accelerate the daytime-restricted feeding-induced phaseshift (Le Minh et al., 2001). In some brain regions, GC rhythm is very important for generation of Per2 rhythm. The brain specific ablation of GR abolished Per2 rhythm in the oval nucleus of the bed nucleus of the stria terminalis and central nucleus of the amygdala, but not in the SCN, basolateral amygdale and dentate gyrus

(Segall et al., 2009). Because the administration of DEX into the SCN-lesioned mice could synchronize about 60% of circadian liver transcriptome, it is likely that GC rhythm widely affect circadian patterns of many types of metabolism (Reddy et al., 2007).

PURPOSE

Synchronization between the master clock and peripheral clocks is an important issue in circadian biology. A strong one among synchronizing signals is glucocorticoid (GC) that is released from the adrenal gland, because it directly regulates circadian clock genes. In Chapter 1, to understand how GC regulates a core clock gene, *Period2* (*Per2*), I explored the molecular mechanisms of GC-evoked *Per2* induction. I was also interested in determining the effects of the abrogated response of *Per2* to GC on the circadian oscillation patterns.

Based on the novel molecular mechanism of GC examined in the study of Chapter 1, I intended to identify the group of GC-responsive genes, of which the GC responsiveness is modulated by the circadian rhythm transcription factor, *Bmal1*. To identify the global regulatory patterns of Bmal1 on GC-responsive genes, I performed the microarray experiment using WT and *Bmal1*$^{-/-}$ mouse embryonic fibroblasts in Chapter 2.

CHAPTER 1.

Glucocorticoid-mediated Period2 induction delays the phase of circadian rhythm

ABSTRACT

Circadian rhythm is an endogenous rhythm of about 24 hr period that regulates overall physiology and behavior. The master clock is resided in the SCN of the hypothalamus and synchronizes the circadian rhythm of peripheral tissues by neural and humoral signals. GC is one of the synchronizing signals that can induce the expression of circadian genes, including *Per2*. In this chapter, I studied the molecular mechanisms of *Per2* induction by GC signaling. I found that GC prominently induced *Per2* expression and delayed the circadian phase. From the sequence analysis of *Per2* promoter, I found the overlapping GRE and E-box that was responsible for GC-mediated *Per2* induction. Interestingly, GRE in *Per2* promoter required BMAL1 for GC responsiveness, whereas other GRE-containing promoters, such as *Per1* and mouse mammary tumor virus (MMTV), responded to DEX in the absence of BMAL1, due to BMAL1-dependent binding of GR to Per2 GRE. When *Per2* could not be induced by the mutation of GRE or E-box, the phase of circadian oscillation failed to be delayed when compared to that of the wild type. Therefore, the present study reveals that GC-mediated *Per2* induction through the novel regulatory mechanism is important for delaying the circadian rhythm.

Key words: circadian rhythm, Period2, Bmal1, glucocorticoid, phase delay

INTRODUCTION

The circadian clock is comprised of an endogenous rhythm that provides approximate 24-hr timing cues to various biological activities, including metabolism, physiological processes, and behavior. In mammals, the master pacemaker resides in the SCN of the hypothalamus. The SCN has self-sustainable oscillators and synchronizes the circadian timing of peripheral tissues by transmitting neuronal and humoral signals. Peripheral tissues also have endogenous clock machinery and are thus able to maintain the circadian rhythm without any external cues (Reppert and Weaver, 2002; Welsh et al., 2010).

The endogenous circadian timing system consists of molecular feedback mechanisms, including the core and auxiliary loop. In the core loop, two bHLH–PAS-containing transcription factors, CLOCK and BMAL1 bind to the E-box of clock-controlled genes, such as *Per 1/2*, *Cry 1/2*, *Rev-erbα* and *RORα*. The translated PERs and CRYs translocate to the nucleus and repress CLOCK:BMAL1 activity in order to return to the starting point. The auxiliary loop reinforces the circadian rhythm by regulating the rhythmic expression of BMAL1 through competitive binding of RORα and REV-ERBα to RRE on the *Bmal1* promoter (Dibner et al., 2010; Mohawk et al., 2012).

The endogenous clock does not have an exact 24-hr period and has the flexibility to adjust to the phases of the environmental cycle, especially the light/dark photocycle. Light exposure at the time of early/late subjective night results in a delay/advance of the next activity cycle, which is represented as a phase response curve (PRC). It has been widely accepted that rapid expression of *Per1* and *Per2* plays a crucial role in the light-dependent resetting process. In particular, *Per1* and *Per2* are thought to mainly play a role in phase advance and phase delay, respectively; however, their actual roles only in the resetting process remain to be elucidated (Albrecht et al., 2001; Bae and Weaver, 2003; Cermakian et al., 2001; Pendergast et al., 2010; Wakamatsu et al., 2001). These molecular events also occur in peripheral tissues and immortalized cell lines through synchronizing signals (Balsalobre et al., 2000a; Balsalobre et al., 1998).

GC is a multifunctional hormone that regulates glucose and lipid metabolism, immune activity, the stress response, and learning and memory (Chung et al., 2011; Kassel and Herrlich, 2007; Popoli et al., 2011). The level of GC displays a robust circadian rhythm, and the administration can reset the rhythmic phase of peripheral tissues and immortalized cells (Balsalobre et al., 2000a). Furthermore, the expression of GRs in most peripheral cells, not in the SCN, enables the entrainment of peripheral clocks without any interference of the master clock. Therefore, GC is

considered to be the best candidate for the synchronizing signal between the SCN and peripheral tissues.

During the synchronization process, *Per1* and *Per2* are rapidly induced and oscillate in a circadian fashion. While GC regulates *Per1* through the GRE in its promoter region, the molecular mechanisms of GC-mediated *Per2* expression have not been clearly elucidated (Yamamoto et al., 2005a). ChIP-seq analysis revealed that three GR-binding sites exists near *Per2* gene (Reddy et al., 2009). Several studies have shown that *Per2* promoter region, in which the canonical GRE has not been found, is enough for GC responsiveness to *Per2* (Hattori, 2011; Izumo et al., 2006). On the other hand, So *et al*. reported that the intronic GR-binding sequence (GBS) can confer GC responsiveness to *Per2* (So et al., 2009).

Per2-knockout mice show a significantly shorter circadian rhythm or arrhythmicity of locomotor activities and have defects in the anticipation of feeding (Albrecht et al., 2001; Feillet et al., 2006; Pendergast et al., 2010; Wakamatsu et al., 2001; Zheng et al., 1999). Per2 is not only a component of the circadian oscillator, but also functions as a mediator for the timed regulation of many types of metabolism. Direct interactions between PER2 and various nuclear receptors, including HNF4α, REV-ERBα, and PPARα, enable the circadian oscillation of glucose and lipid metabolism (Schmutz et al., 2010). Besides, *Per2*-knockout mice, which lack 9th intron containing

GC-responsive region, exhibited altered GC-induced glucose intolerance and insulin resistance, partly due to increased leptin levels (So et al., 2009). It is also related to the timing of sleep. *Per2*-knockout mice wake earlier than WT mice, and the human PER2 S662G mutation prevents the phosphorylation of PER2 by CKIε, resulting in rapid degradation and nuclear export, which is observed in patients with familial advanced sleep phase syndrome (FASPS) (Kopp et al., 2002; Toh et al., 2001; Vanselow et al., 2006). Therefore, the exact timing of *Per2* expression may be critical for maintaining or restoring a physiology that is properly attuned to the environmental light-dark cycle.

In the present study, I investigated the molecular mechanisms underlying GC-mediated *Per2* induction and its functional relevance to the regulation of the circadian rhythm. I provide evidence that BMAL1-dependent binding of GR to the overlapping GRE/E-box in the 5′ upstream region of *Per2* gene induces the expression of *Per2*. Furthermore, I demonstrate that GC-mediated *Per2* induction by this BMAL1-dependent GR mechanism is responsible for the phase delay.

MATERIALS AND METHODS

Cell culture

Wild type (WT), Per2::luc knock-in, *Per2*$^{-/-}$, and *Bmal1*$^{-/-}$ mouse embryonic fibroblasts (MEFs) were spontaneously immortalized as previously described (Bae et al., 2001; Bunger et al., 2000; Todaro and Green, 1963a; Yoo et al., 2004). Primary or immortalized cell lines were maintained in Dulbecco's modified Eagle's medium (Invitrogen, Carlsbad, CA, USA) supplemented with 10% fetal bovine serum (FBS) and 1% penicillin/streptomycin at 37°C in a humidified atmosphere containing 5% CO_2.

Constructs

Per2 promoter region from -1671 to +26 from the transcription start site (TSS) was cloned into the GL3-basic vector (Promega, Madison, WI, USA), in which the PEST sequence was inserted into the C-terminal of the luciferase gene. The final construct was called Per2 (-1671)::dsluc. A series of 5′ deletion mutants were prepared from Per2 (-1671)::dsluc. E1, E2, GRE, and palindromic GRE mutants were generated from Per2 (-271)::dsluc by the site-directed mutagenesis using the following primers: E1 mutant up: 5′-

CGGGCTCAGCGCGCGCGGT**GCTAG**TTTCCACTATGTGACAGCGG-3′, E1 mutant dn: 5′-CCGCTGTCACATAGTGGAA**ACTAGC**ACCGCGCGCGC TGAGCCCG-3′; E2 mutant up: 5′-CGGCGAACATGGAGTTC**CATAGA** CGTCTTATGTAAAG-3′, E2 mutant dn: 5′-CTTTACATAAGACG**TCTATG** GAACTCCATGTTCGCCG-3′; GRE mutant up: 5′-GAGGAACCCGGGCGG C**T**A**GT**ATGG**ATA**TCCATGTGCGTCTTATG-3′, GRE mutant dn: 5′-CATAATACGCACATGGA**TAT**CCAT**AC**T**A**GCCGCCCGGGTTCCTC-3′; palindromic GRE up: 5′-GGAACCCGGGCGG**A**GAACATGG**T**GTTC**T**ATGT GCGTCTTATG-3′, palindromic GRE dn: 5′-CATAAGACGCACAT**A**GAAC**A** CCATGTTC**T**CCGCCCGGGTTCC-3′.

Luciferase assay

WT and *Bmal1*$^{-/-}$ MEFs were transfected using Lipofectamine PLUS reagents (Invitrogen). Cells were harvested after treatment with 0.1% ethanol or 1 μM dexamethasone, a synthetic GC (DEX; Sigma-Aldrich, St. Louis, MO, USA), for 10-hr, which elicited the maximal induction. Luciferase activities were analyzed by the dual luciferase reporter assay system (Promega). Fold induction was calculated by dividing the luciferase activities in the DEX-treated group by those in the ethanol-treated group.

Recording of real-time luminescence

Per2::luc knock-in MEFs were cultured the day before the monitoring of luminescence. After treatment with the various compounds (0.1% ethanol, 1 μM DEX, 0.1% DMSO, 10 μM forskolin, 50% horse serum, 1 mM dbcAMP, and 1 μM ionomycin) for 2- hr, and media were changed to normal culture media with 100 μM luciferin (Promega). Per2 (-271)::dsluc and its mutants were transfected into WT MEFs for 24-hr. Bioluminescence was measured for 1 min for each dish at 10 min intervals with a real-time luminescence monitoring device (Kronos-Dio; ATTO Corporation, Tokyo, Japan) at 36°C in a humidified atmosphere containing 5% CO_2. Data were normalized by the average of the initial minimum value.

Real-time RT-PCR

MEFs were seeded in 6 well plates and harvested at the indicated times after treatment with 0.1% ethanol or 1 μM DEX (with or without 5 μM RU486; *Sigma-Aldrich*). Total RNA was isolated by the single-step acid guanidinium thiocyanate-phenol-chloroform method. Next, 2 μg of RNA was reverse-transcribed using Moloney murine leukemia virus reverse transcriptase (Promega). Real-time PCR was carried out in the presence of SYBR Green I. Gene expression levels were normalized to glyceraldehyde-3-phosphate dehydrogenase (GAPDH) levels. The primers used for real-time RT-PCR were as follows: *Per1* up, 5′-GTGTCGTGATTAAATTAGTCAG

-3′, *Per1* dn, 5′-ACCACTCATGTCTGG GCC-3′; *Per2* up, 5′-GCGGATGCTC GTGGAATCTT-3′, *Per2* dn, 5′-GCTCCTTCAGGGTCCTTATC-3′; *GAPDH* up, 5′-CATGGCCTTCCGTGTTCCTA-3′, *GAPDH* dn, 5′-CCTGCTTCACCA CCTTCTTGA-3′.

Chromatin immunoprecipitation

WT and *Bmal1*$^{-/-}$ MEFs were treated with 0.1% ethanol or 1 μM DEX for 1-hr and exposed to 1% formaldehyde for 10 min. Cells were collected and were made to swell with hypotonic buffer (5 mM PIPES, pH 8.0, 85 mM KCl, 0.5% Triton X-100, 1 mM PMSF, 1 mM Na_3VO_4, 1 mM NaF, and protease inhibitor cocktail). After centrifugation, the nuclear pellet was lysed in nuclear lysis buffer (1% Triton X-100, 0.5% sodium deoxycholate, 0.1% SDS, 1 mM PMSF, 1 mM Na_3VO_4, 1 mM NaF, and protease inhibitor cocktail). The chromatin was sheared off by sonication to less than 500 bp. Precleared samples were immunoprecipitated with normal rabbit serum and anti-GR (Santa Cruz Biotechnology, Santa Cruz, CA, USA). The immunoprecipitated DNA was purified with phenol/chloroform. For PCR, the primers were as follows: *Per1* GRE up, 5′-AAGGCTGTGTGCATGTCCT-3′, *Per1* GRE dn, 5′-AGAGGGAGGTGACGTCAAAG-3′; *Per2* GRE up, 5′-GTGCCAGGTGAATGGAAGTC-3′, *Per2* GRE dn, 5′-AGCTACGCTCGTC AATTGGT-3′.

Adenoviral transduction

Per2 recovery constructs were designed to express PER2-LUCIFERASE fusion protein under WT or mutant *Per2* promoter (-271 to +26 from the TSS). Adenoviral constructs were generated according to the manufacturer's instructions (Invitrogen). To determine the effects of the WT or mutant viruses, *Per2*$^{-/-}$ MEFs were seeded in 35-mm culture dishes, and the adenoviruses were added after 24-hr. To analyze the circadian patterns of PER2, we recorded luminescence at 36°C with 5% CO_2 using a real-time luminescence monitoring device after a 2-hr DEX treatment.

Statistical analysis

Data were analyzed by one-way analysis of variance (ANOVA) with Tukey post-hoc tests using GraphPad Prism software (GraphPad Prism Software, Inc., La Jolla, CA, USA). A *p*-value of less than 0.05 was considered to be significant.

RESULTS

GC induces *Per2* expression and delays the circadian phase

Many signaling pathways regulate clock gene expression (Balsalobre et al., 2000b; Izumo et al., 2006). To examine the effects of GC on *Per2* expression, I treated Per2::luc knock-in MEFs with DEX, forskolin, dibutyryl cyclic AMP (dbcAMP), ionomycin, or horse serum and compared the oscillation profiles by recording real-time bioluminescence. DEX significantly increased PER2 protein levels, with a peak at approximately 10-hr after treatment, whereas the other stimuli did not elicit gene expression (Figure 3A). Moreover, the phase of PER2 oscillation was significantly delayed in the DEX-treated group (Figure 3B). To verify the functional role of GR on DEX-mediated *Per2* expression, Per2::luc knock-in MEFs were cotreated with RU486 (a GR antagonist). Both DEX-induced PER2 expression and the delay in phase were completely blocked by RU486 (Figure 3C and D). These results indicated that the intact GR activity was required for the regulation of *Per2* expression and delay in the circadian phase. Consistently, the induction of *Per1* and *Per2* mRNA expression was also blocked by RU486 treatment, indicating that those genes were regulated by GC at the transcriptional level (Figure 3E).

Interestingly, the induction profile of *Per1* expression by DEX occurred more rapidly than that of *Per2*. Moreover, *Per1* expression was elicited by other signals that did not increase *Per2* levels (Figure 4) (Yamamoto et al., 2005a). Hence, although *Per1* and *Per2* are immediate early genes and have a certain redundancy of function in relation to circadian rhythm, they may produce different outputs depending on the combination of different signal transduction pathways activated. These results suggested that GC-induced *Per2* expression was responsible for the phase delay. Therefore, I investigated the molecular mechanism of GC-mediated *Per2* induction and its relevance to the regulation of circadian rhythms.

Identification of the GC-responsive region in the *Per2* promoter

To determine whether GC-induced *Per2* expression was regulated by the promoter region, I compared DEX-stimulated oscillation profiles of Per2::luc knock-in and *Per2* promoter-driven luciferase (Figure 5A). Although the overall profile of Per2::luc knock-in was delayed, compared to that of *Per2* promoter activity, the inductive and circadian oscillatory patterns exhibited very similar profiles. This result indicated that the 5′ upstream region of *Per2* gene was sufficient for DEX-mediated *Per2* induction and circadian oscillation. To narrow down the precise region required for *Per2* induction, I generated serially deleted promoter constructs

(Figure 5B). Although the basal promoter activities of Per2 (-241)::dsluc and Per2 (-201)::dsluc were decreased, the fold induction by DEX treatment was maintained up to Per2 (-201)::dsluc. However, when the region from -201 to -171 was deleted, the fold induction was completely blocked (Figure 5C). These effects were also demonstrated by the recording of real-time bioluminescence. The induction and oscillation profiles of Per2 (-271)::dsluc were almost the same as those of the full length promoter, i.e., Per2 (-1671)::dsluc, but, Per2 (-201)::dsluc and Per2 (-171)::dsluc were not induced (Figure 6). Interestingly, these deletion mutants maintained their circadian oscillations, but without *Per2* induction, implying that distinct mechanisms regulate the induction event and subsequent oscillations.

The conserved region containing the overlapping GRE and E-box is responsible for *Per2* induction

Circadian clock genes are highly conserved in mammals (Emery et al., 1998; Huang et al., 2012; Zylka et al., 1998). To gain insight into the putative role of the GC-responsive region, I compared the 5′ upstream region of *Per2* gene in several mammalian species. The proximal region of *Per2* promoter was conserved in mice, humans, rats, cows, and monkeys (Figure 7). Sequence analysis revealed that the conserved regions contain a D-box, CCAAT-box, GC-box, and a putative GRE, which differed slightly

from the consensus sequence (5′-GGTACANNNTGT(T/C)CT-3′). I also found it to be overlapped with one of E-boxes (E2) by1-bp. To investigate the possibility of interaction between the two elements, I generated mutant constructs of Per2 (-271)::dsluc, the shortest construct exhibiting the same circadian oscillation and DEX responsiveness as the full-length promoter (Figure 9). The basal levels of the GRE mutant (GRE^{mut}) and E1 mutant ($E1^{mut}$) were similar to the WT; however, the E2 mutant ($E2^{mut}$) exhibited increased basal activity. As expected, GRE^{mut} completely blocked responsiveness to DEX. Interestingly, DEX responsiveness was also blocked in $E2^{mut}$, whereas $E1^{mut}$ only partially decreased the fold induction (Figure 7B). These data suggested that the overlapping GRE/E2 (GE2) was crucial for DEX-mediated *Per2* induction and E1 had only a moderate effect on this induction.

To elucidate whether the functional interaction between the GRE and E-box was generally found in GC signalling, I tested the effects of the GRE-E-box interaction on the mechanism of *Per1* induction. While mutations in GREs completely blocked *Per1* induction, mutations in E-boxes did not affect this event (Figure 8). These results indicated that the functional interaction between GRE and E-box, as shown in the *Per2* promoter, was not a general mechanism of GC signaling.

To confirm that E-boxes on the *Per2* promoter were responsible for the

binding of the circadian clock machinery, I examined CLOCK:BMAL1-mediated transcriptional activities of these mutants. $E1^{mut}$ and $E2^{mut}$ partially impaired CLOCK:BMAL1 activities, while GRE^{mut} did not, despite its close proximity to E2 (Figure 7C). These results showed that while both E-boxes had functional roles in CLOCK:BMAL1-mediated transcriptional activity, GRE was not involved in mediating this effect. These results also implied that E-box-mediated transcriptional activity was closely related to GC-induced *Per2* expression.

BMAL1 is essential for GC-mediated *Per2* induction

The functional interaction between the GRE and E-box suggested that BMAL1 might be involved in GC-mediated *Per2* induction. To test this hypothesis, I generated Per2::luc knock-in MEFs of two genotypes (WT and *Bmal1*$^{-/-}$) and compared the circadian profiles of these MEFs after DEX treatment. As shown in Fig. 9A, *Bmal1*$^{-/-}$ MEFs did not show circadian oscillation or responsiveness to DEX. Consistently, *Per2* mRNA was not induced by DEX treatment in *Bmal1*$^{-/-}$ MEFs, while *Per1* mRNA was increased (Figure 9B). To determine whether the abrogation of *Per2* induction in *Bmal1*$^{-/-}$ MEFs might be resulted from *Per2* promoter activities, I performed reporter assays in WT and *Bmal1*$^{-/-}$ MEFs (Figure 9C). While *Per1* promoter-driven luciferase activities were still increased by DEX

treatment in the absence of *Bmal1*, the induction of *Per2* promoter driven-luciferase activity was abolished in *Bmal1*$^{-/-}$ MEFs. To further examine these properties in relation to GRE-dependent mechanisms, I also tested mouse mammary tumor virus (MMTV) promoter activities in WT and *Bmal1*$^{-/-}$ MEFs. Similar to the result in the case of *Per1*, MMTV promoter activities were increased by DEX treatment in *Bmal1*$^{-/-}$ MEFs. These data indicated that BMAL1 was critical for DEX-induced *Per2* expression, and this was distinct from the general GRE mechanism of action.

BMAL1 regulates GR occupancy in the GRE of *Per2* promoter

To further elucidate the effects of GR on *Per2* promoter, I performed a reporter assay with the DNA binding mutant of GR (DBD^{mut}) (Kassel and Herrlich, 2007; Mikuni et al., 2007). DBD^{mut} decreased DEX responsiveness of *Per2*, MMTV, and *Per1* promoters (Figure 10A). To investigate the direct binding of GR to *Per2* promoter region and the role of BMAL1 in *Per2* induction, I performed chromatin immunoprecipitation (ChIP) assays in WT and *Bmal1*$^{-/-}$ MEFs. The recruitment of GR to the GRE in *Per2* promoter was increased by DEX treatment in WT MEFs, but was completely absent in *Bmal1*$^{-/-}$ MEFs (Figure 10B). However, GR occupancy of *Per1* promoter was increased not only in WT MEFs but also in *Bmal1*$^{-/-}$ MEFs. I also analyzed GR occupancy of the GBS in the Per2 intron region (So et al.,

2009). Similar to the effect observed in *Per1* gene, GR occupancy in the intronic GBS of *Per2* gene was increased by DEX treatment in WT and *Bmal1*$^{-/-}$ MEFs. Although the binding of GR to both *Per1* GRE and *Per2* GBS was increased by DEX treatment in both MEFs, the amount of immunoprecipitated DNA in *Bmal1*$^{-/-}$ MEFs was decreased than that in WT MEFs, possibly due to low levels of GR in *Bmal1*$^{-/-}$ MEFs (Figure 11). Consistent with the results of the ChIP assay, GBS-mediated luciferase activities were increased by DEX treatment in WT and *Bmal1*$^{-/-}$ MEFs (Figure 12). These data suggested that BMAL1 was required for the binding of GR to the GRE in *Per2* promoter, but was not critical for the binding of GR to the GBS in Per2 intronic region. Considering the complete absence of *Per2* induction in *Bmal1*$^{-/-}$ MEFs, GE2 in *Per2* promoter was epistatic to the intronic GBS in GC-mediated *Per2* induction.

An imperfect palindromic GRE confers the reliance on the overlapping E-box

The GRE in *Per2* promoter differs from the palindromic GRE sequence by 4 bp (5′-AGAACANNNTGTTCT-3′). It has been reported that GR has a higher binding affinity for the palindromic GRE than for the imperfect palindromic sequence and that the palindromic GRE decreases the need for the activities of accessory factors (Scott et al., 1998). To test the

possibility that the imperfect palindromic sequence of *Per2* GRE leads to dependency on the E-box, I generated palindromic GRE mutants (GRE^{Pal}) with E1 or E2 mutations (Figure 13A). When the *Per2* GRE sequence was replaced with the palindromic sequence, DEX responsiveness was still maintained. Interestingly, additional mutations of E-boxes to GRE^{Pal} ($GRE^{Pal}E1^{mut}$ and $GRE^{Pal}E2^{mut}$) did not decrease the GC responsiveness of *Per2* promoter, although their basal promoter activities were reduced (Figure 13B). This is different from the original *Per2* promoter. Therefore, these results suggested that the imperfect GRE sequence increased the reliance on the transcription factor BMAL1.

In addition, I also swapped two E-boxes to analyze the role of the E-box in the function of the GRE (Figure 13A). The swapped construct showed increased basal activities but maintained the fold induction (Figure 13C). Hence, the sequence of E-box only controlled the basal promoter activity and was not informative for GRE action. Rather, it is likely that the distance between GRE and E-box is an important factor for GE2 elements.

Impaired *Per2* induction cannot delay the circadian phase

To evaluate the physiological relevance of *Per2* induction, I conducted a rescue experiment. First, I examined the oscillation patterns of *Per2* promoter constructs. After stimulation with DEX, all of the reporter

constructs displayed circadian oscillation patterns; however, this induction was not observed in GRE^{mut} or $E2^{mut}$ (Figure 14A). The mutant reporters exhibited a slightly advanced phase compared with the WT reporter, as previously described (Figure 14B) (Akashi et al., 2006; Yamajuku et al., 2010). Using these constructs, I generated adenoviruses expressing the PER2::LUC fusion protein (PER2 REC) driven by WT or mutant promoters (GRE^{mut} and $E2^{mut}$). *Per2*$^{-/-}$ MEFs were recovered by these viruses, and the bioluminescence was recorded after DEX treatment. The PER2 REC^{WT} responded to DEX treatment and exhibited similar profiles to PER2::luc knock-in MEFs. However, PER2 $REC^{GRE\ mut}$ or PER2 $REC^{E2\ mut}$ did not display inductive profiles and failed to exhibit a delay in the circadian phase compared to the WT (Figure 15A and B). Although mutant reporter activities were slightly advanced as compared with WT reporter activity, the functional recovery constructs displayed a more pronounced difference between WT and mutant reporters, indicating that the induction of the PER2 regulated the circadian phase (Figure 14A and B). Therefore, these data suggested that DEX-mediated Per2 induction was a crucial step in determining the phase of the circadian rhythm.

Figure. 3. DEX induced prominent *Per2* induction and the delayed phases of circadian rhythm. (A) Per2::luc knock-in MEFs were treated with the indicated synchronizing signals for 2-hr and bioluminescence was measured. Ethanol (0.1%; sky line), DEX (1μM; black line), DMSO (0.1%; gray line), forskolin (10μM; green line), dbcAMP (1mM; dark cyan line), ionomycin (1μM; purple line), medium change (mustard-colored line), and serum shock (medium containing 50% horse serum; red line). (B) The phase of the second peak was measured for all stimuli in (A) (*, $P<0.05$; n=3). (C) PER2::luc knock-in MEFs were treated with RU486 (5μM) in combination with DEX for 2-hr. Ethanol (sky line), DEX (black line), RU486 (pink line), RU486 + DEX (dark red line). (D) The phase of the second peak was measured for all stimuli in (B) (*, $P<0.05$; n=4). (E) WT MEFs were treated with ethanol or DEX for 2-hr with or without RU486. Cells were harvested at the indicated times, and *Per1* and *Per2* mRNA levels were analyzed using real-time PCR. Each value was normalized to the GAPDH expression level (n=4). Values are the mean ± standard error of the mean (SEM) of three or four independent experiments performed in triplicates.

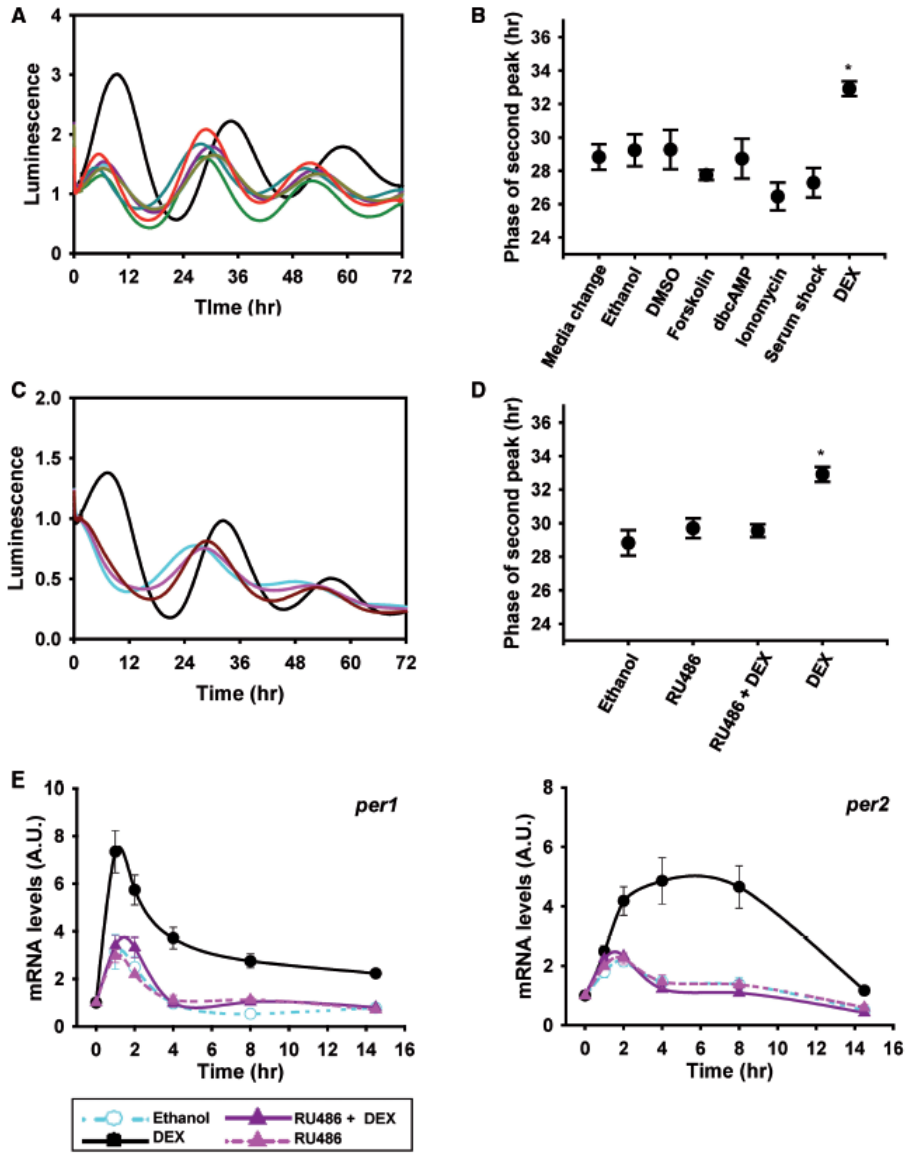
A
Luminescence
Time (hr)
B
Phase of second peak (hr)
Media change
Ethanol
DMSO
Forskolin
dbcAMP
Ionomycin
Serum shock
DEX
C
Luminescence
Time (hr)
D
Phase of second peak (hr)
Ethanol
RU486
RU486 + DEX
DEX
E
per1
per2
mRNA levels (A.U.)
Time (hr)
Ethanol
DEX
RU486 + DEX
RU486

Figure. 4. Acute responses of *Per1* promoter to treatment with several compounds. WT MEFs were transfected with Per1-dsluc and treated with ethanol (0.1%; dotted line), DEX (1μM; solid line), DMSO (0.1%; short dashed line), forskolin (10μM; long dashed line), or ionomycin (1μM; dash-dot-dot line) continuously during the real-time luminescence recording.

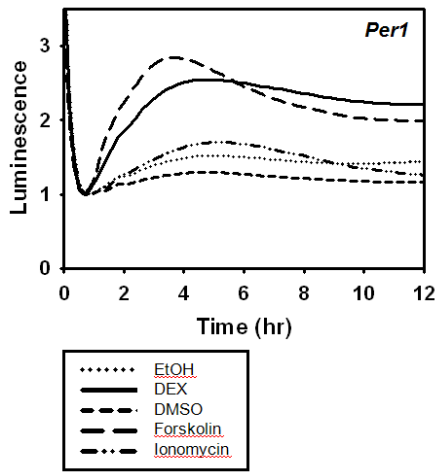
Per1
Luminescence
0
1
2
3
0
2
4
6
8
10
12
Time (hr)
EtOH
DEX
DMSO
Forskolin
Ionomycin

Figure. 5. Serial deletion analysis of the mouse *Per2* promoter. (A) Comparison of the bioluminescence profiles after DEX treatment between the Per2::luc knock-in MEFs (left) and WT MEFs, which were transfected with *Per2* promoter driven-luciferase of approximately 1.7 kbp (right). (B) Schematic diagram of the mouse *Per2* promoter serial deletion constructs. Nucelotides are numbered from the transcription start site. (C) DEX-responsiveness was analyzed in *Per2* serial deletion mutants. WT MEFs were transfected with the serial deletion mutants and treated with ethanol (0.1%; white bar) or DEX (1μM; black bar) for 10-hr, which elicited maximal *Per2* induction (left). Fold induction was calculated by dividing the luciferase activities in the DEX-treated group with those in the ethanol-treated group (right). Values are the mean ± standard error of the mean (SEM) of three independent experiments performed in triplicates (*, $P<0.05$; **, $P<0.01$).

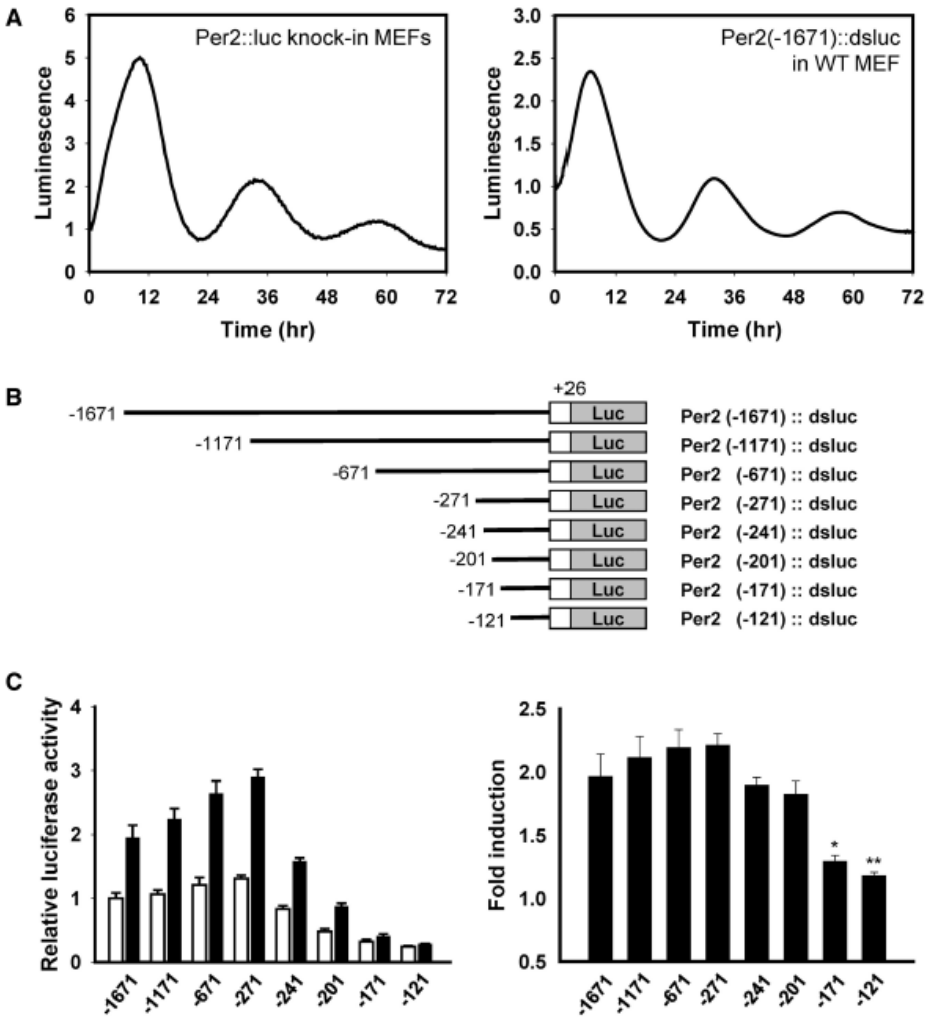
A
Per2::luc knock-in MEFs
Luminescence
Time (hr)
Per2(-1671)::dsluc
in WT MEF
B
+26
Luc
-1671
-1171
-671
-271
-241
-201
-171
-121
Per2 (-1671) :: dsluc
Per2 (-1171) :: dsluc
Per2 (-671) :: dsluc
Per2 (-271) :: dsluc
Per2 (-241) :: dsluc
Per2 (-201) :: dsluc
Per2 (-171) :: dsluc
Per2 (-121) :: dsluc
C
Relative luciferase activity
Fold induction
*
**

Figure. 6. Circadian oscillation patterns of *Per2* promoter serial deletion mutants. WT MEFs were transfected with *Per2* promoter serial deletion mutants: Per2 (-1671)::dsluc, Per2 (-271)::dsluc, Per2 (-201)::dsluc, or Per2 (-171)::dsluc. After 2-hr DEX (1μM) treatment, *Per2* promoter activities were recorded by the real-time luminescence monitoring.

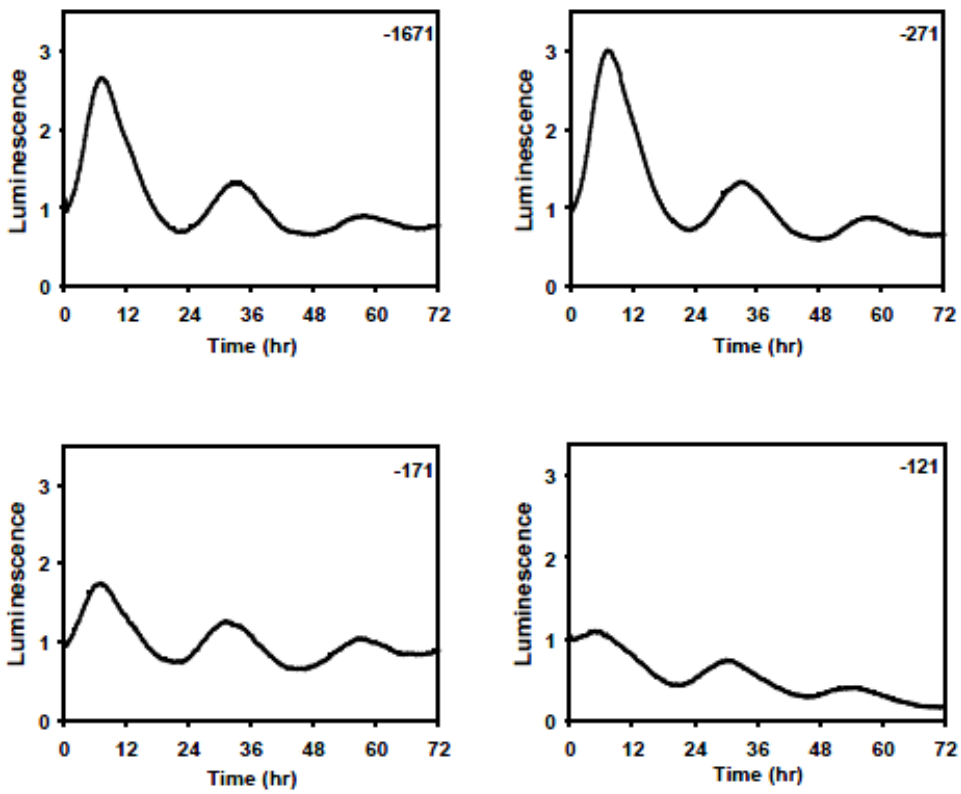
-1671
-271
-171
-121
Luminescence
Time (hr)
0
1
2
3
0
12
24
36
48
60
72

Figure. 7. Both GRE and E-box were required for *Per2* induction. (A) Sequence alignment of the proximal *Per2* promoter region of some mammalian species, including mouse (*M. musculus*), human (*H. sapiens*), rat (*R. norvegicus*), cow (*B. Ttaurus*), and monkey (*M. mulatta*). The conserved regions are shaded gray. Several putative *cis*-elements are indicated, and two E-boxes are named E1 and E2. The asterisk indicates the mutated base. (B) DEX-responsiveness of GRE and E-box mutants. WT MEFs were transfected with WT or mutant constructs and treated with ethanol (0.1%; white bar) or DEX (1μM; black bar) for 10-hr (left). Fold induction was calculated by dividing the luciferase activities in the DEX-treated group with those in the ethanol-treated group (right). (C) CLOCK:BMAL1-mediated transcriptional activation of GRE and E-box mutants. Fold induction was calculated by dividing the luciferase activities in CLOCK:BMAL1-transfected group (black bar) with those in pcDNA3-transfected group (white bar). Values are the mean ± standard error of the mean (SEM) of three independent experiments performed in quadruplicates (***, $P<0.001$).

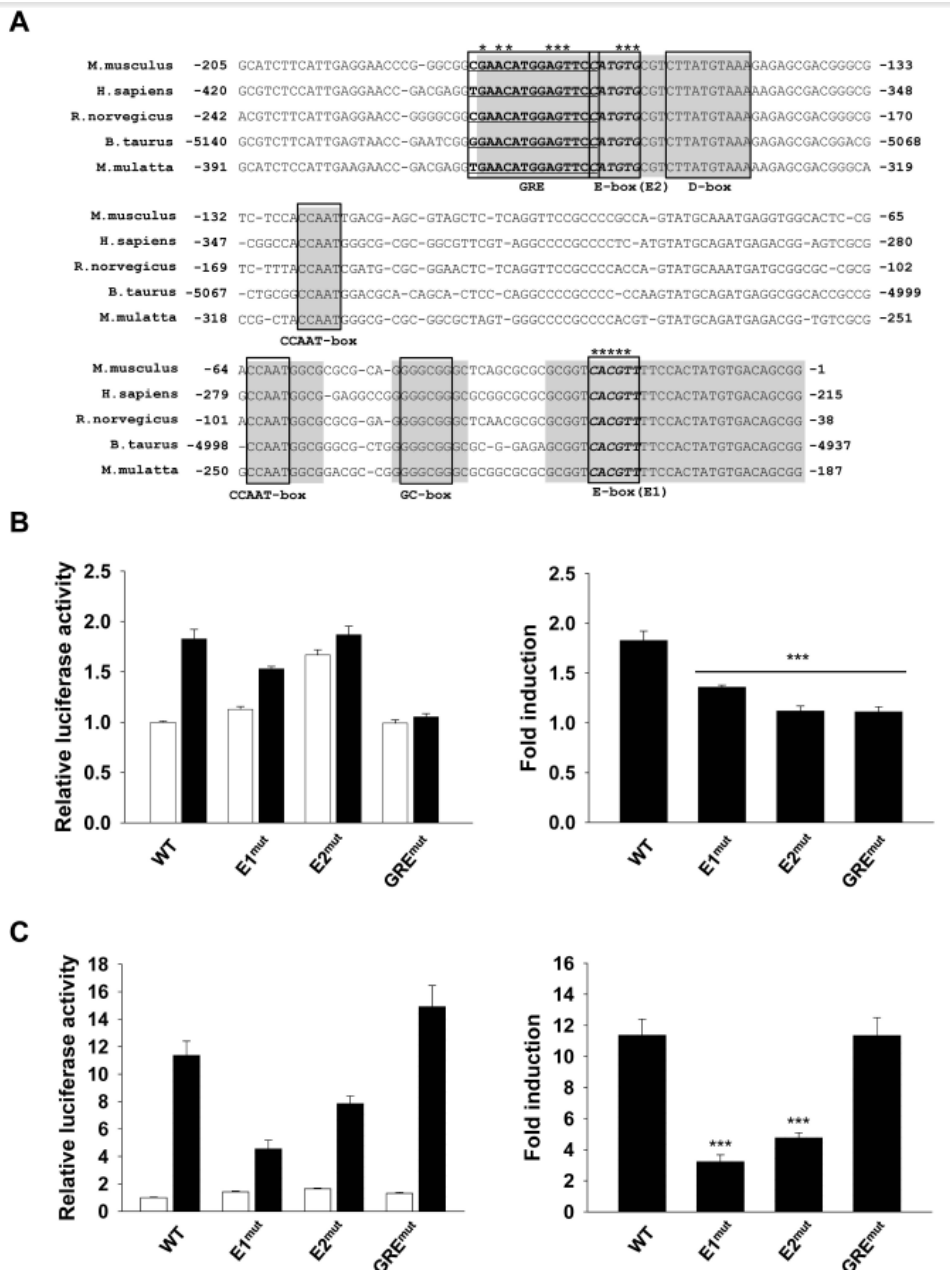
A
M.musculus -205 GCATCTTCATTGAGGAACCCG-GGCGGCGAACATGGAGTTCCATGTGCGTCTTATGTAAAGAGAGCGACGGGCG -133
H.sapiens -420 GCGTCTCCATTGAGGAACC-GACGAGGTGAACATGGAGTTCCATGTGCGTCTTATGTAAAAAGAGCGACGGGCG -348
R.norvegicus -242 ACGTCTTCATTGAGGAACC-GGGGCGGCGAACATGGAGTTCCATGTGCGTCTTATGTAAAGAGAGCGACGGGCG -170
B.taurus -5140 GCGTCTTCATTGAGTAACC-GAATCGGGGAACATGGAGTTCCATGTGCGTCTTATGTAAAGAGAGCGACGGACG -5068
M.mulatta -391 GCATCTCCATTGAAGAACC-GACGAGGTGAACATGGAGTTCCATGTGCGTCTTATGTAAAAAGAGCGACGGGCA -319
GRE
E-box(E2)
D-box
M.musculus -132 TC-TCCACCAATTGACG-AGC-GTAGCTC-TCAGGTTCCGCCCCGCCA-GTATGCAAATGAGGTGGCACTC-CG -65
H.sapiens -347 -CGGCCACCAATGGGCG-CGC-GGCGTTCGT-AGGCCCCGCCCCTC-ATGTATGCAGATGAGACGG-AGTCGCG -280
R.norvegicus -169 TC-TTTACCAATCGATG-CGC-GGAACTC-TCAGGTTCCGCCCCACCA-GTATGCAAATGATGCGGCGC-CGCG -102
B.taurus -5067 -CTGCGGCCAATGGACGCA-CAGCA-CTCC-CAGGCCCCGCCCC-CCAAGTATGCAGATGAGGCGGCACCGCCG -4999
M.mulatta -318 CCG-CTACCAATGGGCG-CGC-GGCGCTAGT-GGGCCCCGCCCCACGT-GTATGCAGATGAGACGG-TGTCGCG -251
CCAAT-box
M.musculus -64 ACCAATGGCGCGCG-CA-GGGGCGGGCTCAGCGCGCGCGGTCACGTTTCCACTATGTGACAGCGG -1
H.sapiens -279 GCCAATGGCG-GAGGCCGGGGCGGGCGCGGCGCGCGGGTCACGTTTCCACTATGTGACAGCGG -215
R.norvegicus -101 ACCAATGGCGCGCG-GA-GGGGCGGGCTCAACGCGCGGGTCACGTTTCCACTATGTGACAGCGG -38
B.taurus -4998 -CCAATGGCGGGCG-CTGGGGGCGGGCGC-G-GAGAGCGGTCACGTTTCCACTATGTGACAGCGG -4937
M.mulatta -250 GCCAATGGCGGACGC-CGGGGGCGGGCGCGGCGCGCGGTCACGTTTCCACTATGTGACAGCGG -187
CCAAT-box
GC-box
E-box(E1)
B
Relative luciferase activity
Fold induction
WT
E1mut
E2mut
GREmut
C
Relative luciferase activity
Fold induction
WT
E1mut
E2mut
GREmut

Figure. 8. DEX responsiveness of Per1 did not depend on E-box. (A) Schematic diagram of *Per1* promoter constructs. (B) WT or mutant constructs (GRE or E-box mutant) of the *Per1* promoter were transfected into WT MEFs. Cells were harvested after treatment with ethanol (0.1%) or DEX (1μM) for 10-hr. Luciferase activities were normalized to renilla luciferase activities, and the fold induction was calculated as the ratio of the value of the DEX-treated group versus that of the ethanol-treated group. Values are the mean ± standard error of the mean (SEM) of three or four independent experiments performed in triplicates (*, $P<0.05$).

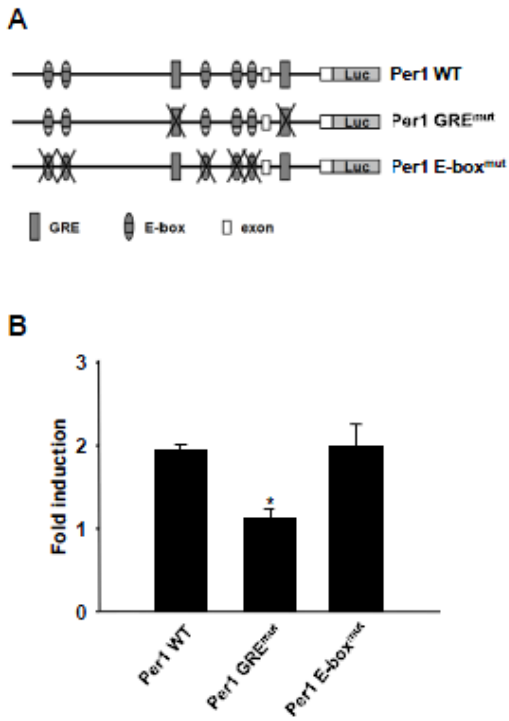
A
Luc
Per1 WT
Per1 GREmut
Per1 E-boxmut
GRE
E-box
exon
B
Fold induction
3
2
1
0
*
Per1 WT
Per1 GREmut
Per1 E-boxmut

Figure 9. BMAL1 was necessary for *Per2* induction. (A) Per2::luc knock-in MEFs with a WT (left) or *Bmal1*$^{-/-}$ (right) genetic background. Bioluminescence was recorded after DEX (1μM) treatment. (B) WT and *Bmal1*$^{-/-}$ MEFs were treated with ethanol (0.1%) or DEX (1μM) for 2-hr. Cells were harvested at the indicated times and *Per1* and *Per2* mRNA levels were analyzed by real-time PCR. Each value was normalized to the GAPDH expression level (n=4). (C) Per1-luc, Per2-luc, and MMTV-luc were transfected into WT (black bar) or *Bmal1*$^{-/-}$ MEFs (white bar), and cells were treated with ethanol (0.1%) or DEX (1μM) for 10-hr. Luciferase activities were normalized to the renilla luciferase activities, and the fold induction was calculated by dividing the luciferase activities in DEX-treated group with those in ethanol-treated group (n=3). Values are the mean ± standard error of the mean (SEM) of three or four independent experiments performed in triplicates.

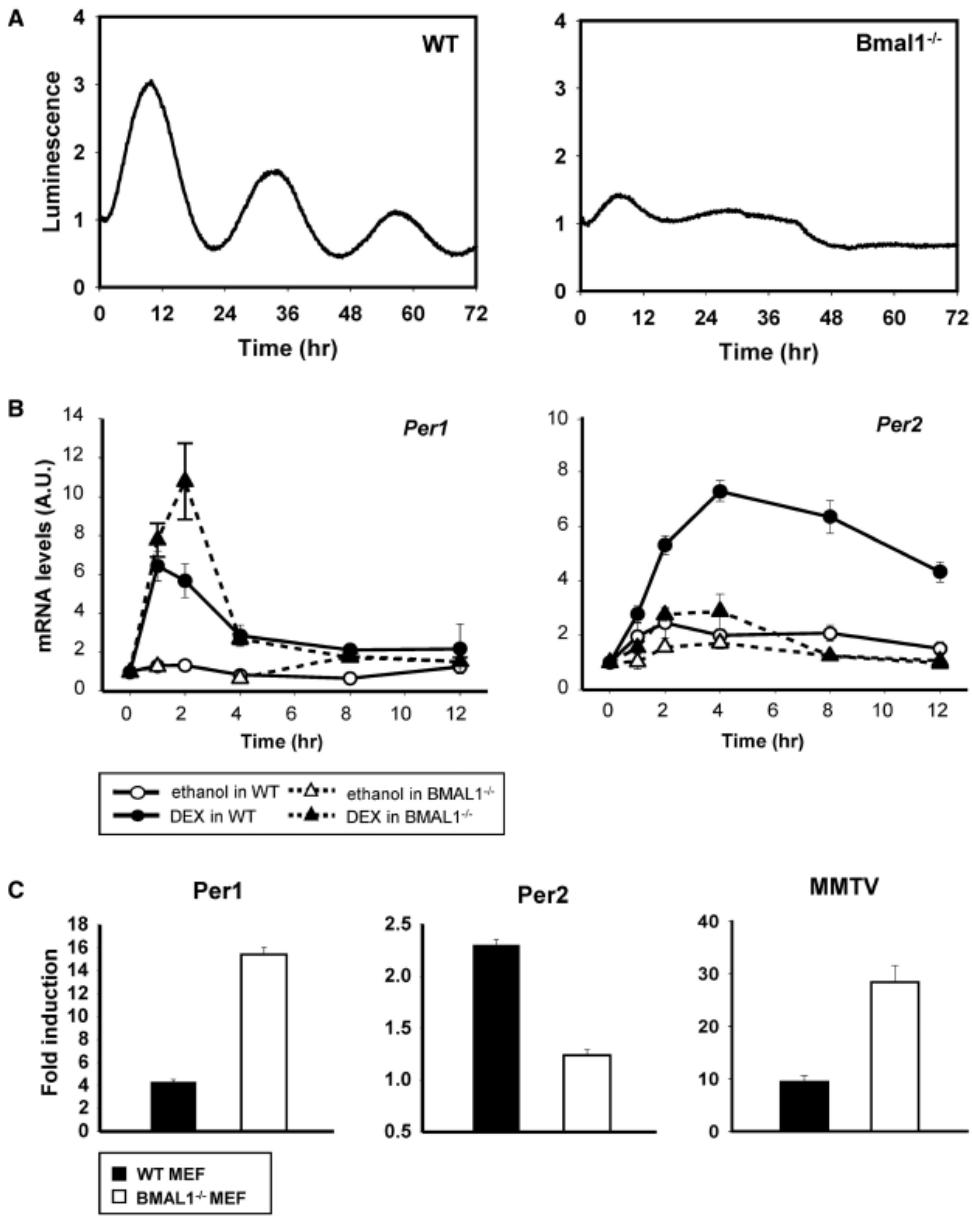
A
WT
Bmal1-/-
Luminescence
Time (hr)
B
Per1
Per2
mRNA levels (A.U.)
Time (hr)
ethanol in WT
ethanol in BMAL1-/-
DEX in WT
DEX in BMAL1-/-
C
Per1
Per2
MMTV
Fold induction
WT MEF
BMAL1-/- MEF

Figure 10. BMAL1-dependent binding of GR to *Per2* promoter. (A) WT GR or DBD^{mut} with MMTV-luc, Per1-luc, and Per2-luc were transfected into WT MEFs. Cells were treated with ethanol (0.1%; white bar) or DEX (1μM; black bar) for 10-hr. Luciferase activities were normalized to renilla luciferase activities. Values are the mean ± standard error of the mean (SEM) of three independent experiments performed in triplicates. (B) WT and *Bmal1*$^{-/-}$ MEFs were treated with ethanol (0.1%; VEH) or DEX (1μM; DEX) for 1-hr. Chromatin was extracted from the harvested cells, and chromatin immunoprecipitation assays were performed with normal rabbit serum (NRS) or anti-GR. Immunoprecipitated DNA was analyzed using the primer sets for Per1 GRE, Per2 GRE and Per2 GBS. Enrichment of GR binding was measured by the agarose gel electrophoresis (upper panel) and quantified by real-time PCR (lower panel). Values are the mean ± standard error of the mean (SEM) of three independent experiments (***, $P<0.001$).

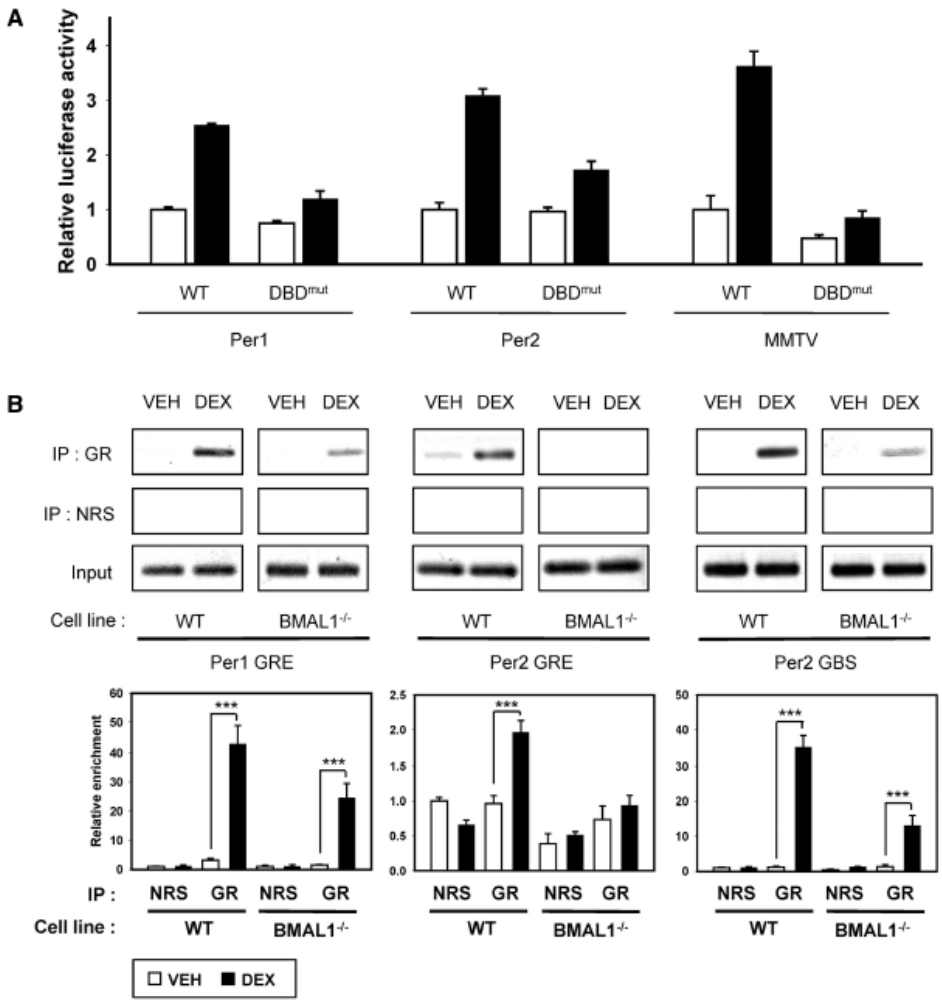
A
Relative luciferase activity
0
1
2
3
4
WT
DBDmut
WT
DBDmut
WT
DBDmut
Per1
Per2
MMTV
B
VEH DEX VEH DEX
VEH DEX VEH DEX
VEH DEX VEH DEX
IP : GR
IP : NRS
Input
Cell line :
WT
BMAL1-/-
WT
BMAL1-/-
WT
BMAL1-/-
Per1 GRE
Per2 GRE
Per2 GBS
Relative enrichment
***
***
***
***
***
***
IP :
NRS GR NRS GR
NRS GR NRS GR
NRS GR NRS GR
Cell line :
WT
BMAL1-/-
WT
BMAL1-/-
WT
BMAL1-/-
VEH
DEX

Figure 11. Decreased GR levels in *Bmal1*$^{-/-}$ MEFs. WT and *Bmal1*$^{-/-}$ MEFs were harvested after treatment with ethanol (V; 0.1%) or DEX (D; 1μM) for 1-hr. Western blot analysis was performed using GR, BMAL1, and β-TUBULIN antibodies.

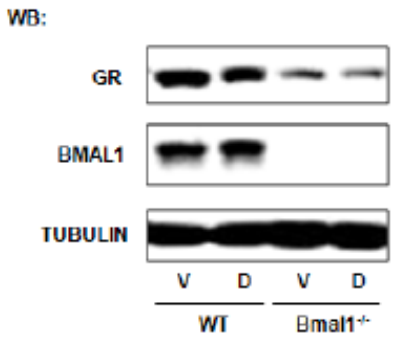
WB:
GR
BMAL1
TUBULIN
V
D
V
D
WT
Bmal1-/-

Figure 12. GBS responded to DEX in the absence of BMAL1. (A) The intron region containing GBS was subcloned into an SV40 promoter driven-luciferase (GBS-SV40P). (B) This construct was transfected into WT and *Bmal1*$^{-/-}$ MEFs, and cells were harvested after treatment with ethanol (0.1%) or DEX (1μM) for 10-hr. Luciferase activities were normalized to renilla luciferase activities, and the fold induction was calculated as the ratio of the value of the DEX-treated group versus that of the ethanol-treated group. Values are the mean ± standard error of the mean (SEM) of three or four independent experiments performed in triplicates.

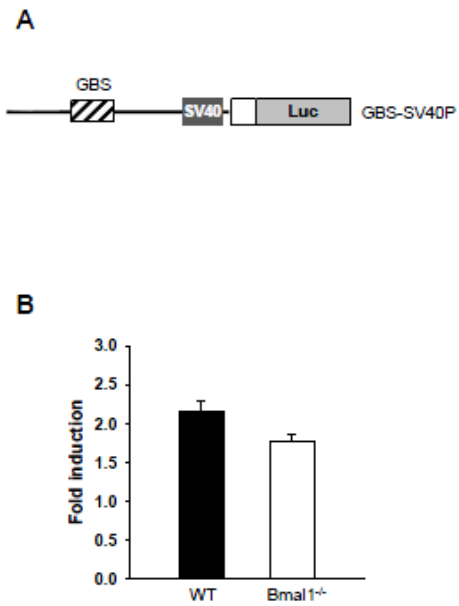
A
GBS
SV40
Luc
GBS-SV40P
B
Fold induction
3.0
2.5
2.0
1.5
1.0
0.5
0.0
WT
Bmal1-/-

Figure 13. The effects of the palindromic GRE and swapped E-boxes on GC-mediated *Per2* induction. (A) Schematic diagram of *Per2* promoter mutants. (B,C) DEX-responsiveness of *Per2* promoter mutants indicated in (A). WT MEFs that were transfected with the reporters were treated with ethanol (0.1%) or DEX (1μM) for 10-hr. Fold induction was calculated by dividing the luciferase activities in the DEX-treated group with those in the ethanol-treated group. Data are represented as the mean ± standard error of the mean (SEM). Three independent experiments were done in triplicates for each condition.

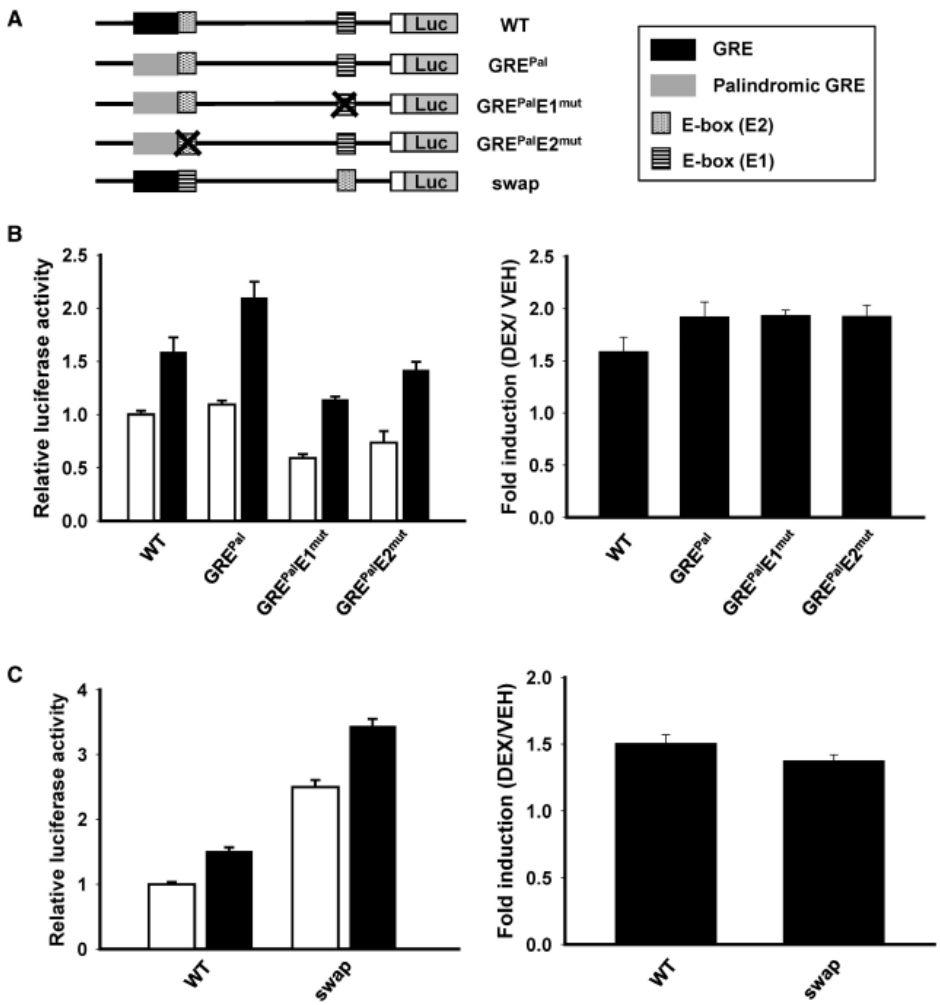
A
Luc
WT
GRE^Pal
GRE^PalE1^mut
GRE^PalE2^mut
swap
GRE
Palindromic GRE
E-box (E2)
E-box (E1)
B
Relative luciferase activity
Fold induction (DEX/ VEH)
WT
GRE^Pal
GRE^PalE1^mut
GRE^PalE2^mut
C
Relative luciferase activity
Fold induction (DEX/VEH)
WT
swap

Figure 14. Circadian oscillation patterns of *Per2* induction mutant reporters. (A) WT or *Per2* induction mutant reporters (GRE^{mut} or $E2^{mut}$) were transfected into WT MEFs. Cells were treated with DEX (1μM) for 2-hr, and bioluminescence was recorded by the real-time luminescence monitoring. (B) The phase of the second peak was measured for WT and *Per2* induction mutant reporters. Values are the mean ± standard error of the mean (SEM) of three or four independent experiments performed in triplicates.

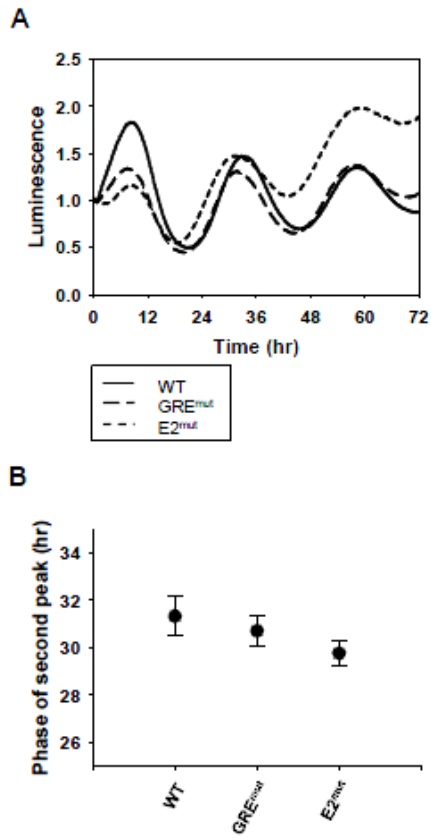
A
2.5
2.0
1.5
1.0
0.5
0.0
Luminescence
0
12
24
36
48
60
72
Time (hr)
WT
GRE^mut
E2^mut
B
34
32
30
28
26
Phase of second peak (hr)
WT
GRE^mut
E2^mut

Figure 15. *Per2* induction mutants cannot delay the circadian rhythm

(A) *Per2*$^{-/-}$ MEFs were recovered with Per2 adenoviruses, in which the expression of *Per2* was regulated by its own promoter. WT (Per2 REC^{WT}; solid line), GRE mutant (Per2 REC$^{GRE\ mut}$; long dashed line), E2 mutant (Per2 REC$^{E2\ mut}$; short dashed line). Bioluminescence was recorded after 2-hr of DEX treatment. (B) The phase of the second peak was measured (**, P<0.01; n=3). Data are represented as the mean ± standard error of the mean (SEM) from three independent experiments.

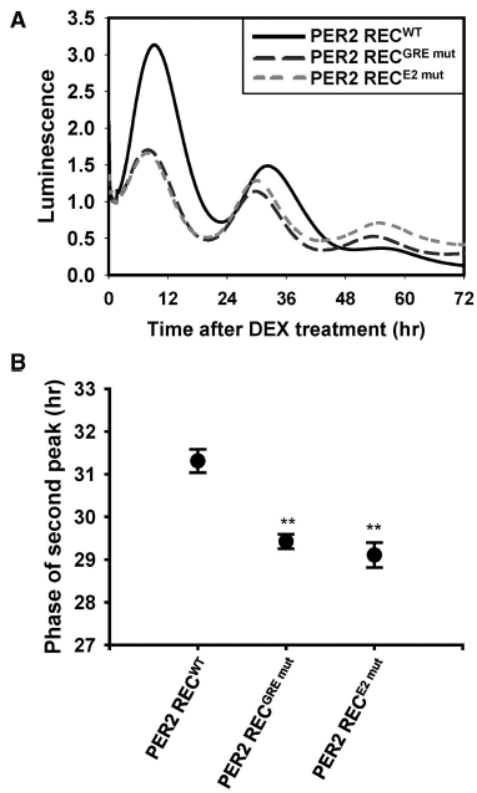
A
Luminescence
3.5
3.0
2.5
2.0
1.5
1.0
0.5
0.0
PER2 REC^WT
PER2 REC^GRE mut
PER2 REC^E2 mut
0
12
24
36
48
60
72
Time after DEX treatment (hr)
B
Phase of second peak (hr)
33
32
31
30
29
28
27
**
**
PER2 REC^WT
PER2 REC^GRE mut
PER2 REC^E2 mut

DISCUSSION

In Chapter I, I investigated the molecular mechanisms of *Per2* induction by GC signaling and its regulatory effects on circadian rhythms. The induction of *Per2* expression by DEX was mainly mediated by the overlapping GRE and E-box (GE2). From our understanding of this molecular mechanism, I demonstrated that *Per2* induction was crucial for delaying the circadian phase.

Among the clock proteins, the fluctuation of PER expression is thought to be crucial for generating circadian oscillation (Chen et al., 2009; Lee et al., 2011; Numano et al., 2006; Yamamoto et al., 2005b). In this regard, it is expected that the resetting process requires an alteration in PER expression in order to generate new rhythms at the initial stage. In fact, various resetting stimuli increase *Per1* and *Per2* levels, while other resetting signals, such as glucose and exercise, lower their expression, respectively, both *in vitro* and *in vivo* (Hirota et al., 2002; Maywood et al., 1999; Yannielli et al., 2002). Several studies have endeavoured to substantiate the importance of the induction of *Per1* and *Per2* in the light-induced phase resetting using *Per1*- or *Per2*-knockout mice, but the exact roles of *Per1* and *Per2* in the resetting process remain controversial. This inconsistency may arise from the fact that the mutant mice used by the

research groups were different, and global *Per*-knockout mice have additional defects besides resetting function defects (Albrecht et al., 2001; Bae and Weaver, 2003; Cermakian et al., 2001; Wakamatsu et al., 2001). Thus, to understand the functional importance of the rapid response of *Per1* and *Per2*, only the specific site responsible for the resetting signal should be mutated. In this respect, the present study attempted to clarify the molecular mechanisms of *Per2* induction and thereby investigate the precise roles of the initial response of *Per2* in the regulation of subsequent circadian rhythms.

GC-induced *Per2* expression was unique in that it required the additional transcription factor BMAL1 for the binding of the GR to the GE2 element. Previous studies revealed that GRE activity was interrupted by other overlapping transcription factor binding sites. For instance, the GRE in the *osteocalcin* gene promoter, which overlaps with all the sequences of the TATA boxes, blocks the binding of the general transcription factor IID and represses transcription (Strömstedt et al., 1991). In a case similar to that of *Per2,* the cAMP-responsive element (CRE) and E-box (CRE/E-box) of the *cyclooxygenase-2* (*COX-2*) gene overlap by 2 bp. Endotoxin-induced *COX-2* gene expression accompanies the activity of the CRE/E-box, in which each element induces a higher level of gene expression than the overlapped sequence (Calomme et al., 2004). In contrast, neither GRE nor

E2 of *Per2* responded to DEX alone, and only their interaction induced *Per2* expression (Figure 7B). To the best of our knowledge, this is the first report of a positive regulatory mechanism, in which the GRE overlaps with other transcription factor binding elements. From a structural viewpoint, this mechanism suggests the cooperative binding of overlapping elements. A previous study showed that GR binds to CLOCK in a ligand-dependent manner, and I also observed direct binding of BMAL1 and GR (data not shown), indicating that the physical interaction between GR and CLOCK/BMAL1 heterodimer can occur (Nader et al., 2009). However, these data cannot answer the question of how this mechanism applied to GE2 on *Per2* promoter. Due to the immediate vicinity of GRE and E2 elements, it is likely that BMAL1 and GR do not bind to GE2 at the same time, but instead do sequentially. Nevertheless, there still exists the possibility that the inherent GRE sequence in *Per2* promoter enables the transcription factors to bind at the same time (Meijsing et al., 2009). To clarify this structural issue, further studies are needed.

Moreover, this mechanism differs from the general GRE action. A previous report suggested that the canonical GRE activity is repressed by CLOCK:BMAL1 through the histone acetyl transferase activities of CLOCK, and consistent with this, I found that the MMTV or *Per1* promoter can respond to DEX, regardless of the activity of BMAL1 (Figure 9A) (Nader et

al., 2009). In contrast, *Per2* cannot be induced in the absence of BMAL1, implying that this mechanism clearly distinct from the canonical GRE mechanism. It is possible that the imperfect palindromic GRE sequence in *Per2* promoter increases the need for the involvement of other transcription factors (Figure 10B). In fact, many genes have GRE and E-box *in tandem* (Reddy et al., 2007). This suggests that these genes are regulated in a gene-specific manner according to the fidelity of the sequences and the distance between the GRE and E-box.

The previous report suggested that the activation of CLOCK:BMAL1 is involved in serum shock-induced *Per1* expression (Jung et al., 2003; Shim et al., 2007). Moreover, the present study revealed that BMAL1 was necessary in GC-mediated *Per2* induction. Therefore, the studies reported by our group suggest that the CLOCK:BMAL1 heterodimer regulates several pathways involved in the resetting process, although it is mainly shown to be a positive regulator of circadian clock genes. Furthermore, each of the resetting signals is likely to generate diverse phases of the circadian rhythm by modulating the expression levels of *Per1* and *Per2* according to the gene-specific functional interaction between the CLOCK:BMAL1 heterodimer and the specific mediator of the resetting signals, such as GR and CRE-binding protein (CREB) (Travnickova-Bendova et al., 2002).

Previous studies have reported that the regulation of circadian timing is achieved by a fine-tuning of circadian clock components at the transcriptional level. At least three *cis*-elements, including the morning-time element (E-box), day-time element (D-box), and night-time elements (RRE), are thought to control this timing. For instance, the peak expression of *Cry1*, which is adjusted by the combinatorial regulation of D-box and RRE in addition to E-box, exhibits a certain delay relative to that of *Per2*, which is mainly controlled by E-box (Ueda et al., 2005; Ukai-Tadenuma et al., 2008; Ukai-Tadenuma et al., 2011). Furthermore, I propose that GRE is another regulatory element involved in the modulation of circadian timing. It is thought that when the resetting stimuli, i.e., GC, is given, the cooperative interaction between GRE and E-box determines the phase of *Per2*. Indeed, the phase-delaying role of E2 has been previously suggested in several studies. Akashi *et al*. reported that the proximal *Per2* promoter region consists of a phase-delaying region and an oscillation-driving region. Using a serial deletion analysis of the *Per2* promoter, they found that the phase-delaying region comprises from -386 to -106 from the TSS and that the oscillation-driving region comprises a region from -105 to +1 (Akashi et al., 2006). The oscillation-driving region contains a non-canonical E-box (E1), which is an essential and sufficient element for the generation of rhythm, while the phase-delaying region contains GE2 (Yoo et al., 2005). Yamajuku

et al. demonstrated similar results in that the region from -161 to -143, which contains E2, was shown to be responsible for the phase delay (Yamajuku et al., 2010). Although they used different stimuli (i.e., serum shock and dbcAMP), the E2-containing region was thought to be responsible for the phase delay. Consistent with this, I also found that $E2^{mut}$ advances the circadian rhythm of *Per2* in DEX-treated cells. Therefore, on the basis of my data and previous studies, DEX-dependent induction of *Per2* expression likely accompanies the long-lasting activation of GE2.

Although the mutated recovery constructs failed to delay the circadian rhythm, the phase difference between the WT and mutant constructs was not as large as that of Per2::luc knock-in cells, which were treated with DEX and other signalling molecules (Figure 3A and 15A). There are a number of plausible reasons for this. First, clock genes other than *Per2* can affect the resetting process. Previous studies reported that GC induces *Per1* expression and downregulates *Rev-erbα* (Torra et al., 2000; Yamamoto et al., 2005a). Although I found that *Per1* expression, which was stimulated by different signaling molecules, did not exhibit remarkable differences between treatments, there was a slight time lag between the stimuli, that may support the phase delaying effect (Figure 4) (Balsalobre et al., 2000b). GC-induced down-regulation of *Rev-erb α* can also directly or indirectly affect phase regulation. Second, it is likely that the excluded region in our

recovery constructs was involved in this mechanism. A previous report showed that *Per2* induction does not occur in *Per2*^{Brdm1} cells, which lack a genomic region of approximately 2 kb containing a GBS; however, my constructs did not contain a GBS (So et al., 2009). Therefore, it is feasible that *Per2* induction may be collectively regulated by the interaction between the two elements, GE2 and GBS. To accurately understand how GE2 and GBS regulate GC-mediated *Per2* induction, further studies need to be conducted using modified BAC clones or the whole genome.

The proximal *Per2* promoter region is highly conserved in mammals and zebrafish (Vatine et al., 2009). This region includes a non-canonical E-box (E1) that is sufficient for self-sustained circadian rhythm generation and D-box that is implicated in higher amplitude generation (Yamajuku et al., 2010; Yoo et al., 2005). In addition, I found that GE2 in this region is also conserved in mammals, but only 5 bp (CATGG) in the middle of the GRE sequence is conserved in zebrafish (Vatine et al., 2009). Although zebrafish has a hypothalamic-pituitary-interrenal (HPI) axis that regulates cortisol release in fish, its exact role in the circadian rhythm remains largely unknown. Considering that its peripheral cells can respond to the light directly and that the zebrafish *Per2* rhythm depends on the LD cycle, it is conceivable that the GC-regulated *Per2* induction mechanism evolved because peripheral tissues do not receive direct photic input (Tamai et al.,

2005).

Many people suffer from sleep disturbances, as well as metabolic and cardiovascular disorders in relation to chronobiological problems that arise under various circumstances, including jet lag and shift work. These disturbances are related to phase misalignment in the master and/or peripheral clocks (Harrington, 2010; Kolla and AUGER, 2011; Park et al., 2011). GC is generally accepted as a strong synchronizer of the SCN and peripheral tissues, and an altered GC rhythm is closely related to a variety of circadian disorders. People suffering from Cushing syndrome, diabetes, depression, obesity, Alzheimer's disease, and metabolic syndrome exhibit an altered GC rhythm and abnormal circadian (Cermakian et al., 2011; Chung et al., 2011; Dickmeis, 2009; Herichova et al., 2005; Tahira et al., 2011).. This might be due to a dysregulation of GC-regulated clock genes, including *Per1* and *Per2* (Barclay et al., 2012).

In conclusion, this study provides evidence that *Per2* induction is responsible for circadian phase delay through a novel regulatory mechanism. It is expected that these findings will help in the effort to achieve a better understanding of the physiological changes that occur in circadian rhythm disorders.

CHAPTER 2.

The global regulatory feature of Bmal1 on glucocorticoid-responsive genes

ABSTRACT

Glucocorticoid (GC) hormone regulates the expression of target genes through the direct binding of the activated GR to the GRE. This action mechanism can be modulated by other transcription factors according to the promoter context. In the present study, I investigated the global regulatory patterns of Bmal1, which is a circadian transcription factor, on GC-responsive genes. From the microarray data analyses by 2-way ANOVA, I found that more than half of GC-responsive genes exhibited different GC-responsiveness in *Bmal1*$^{-/-}$ MEFs. Among Bmal1-modulated GC-responsive genes, most of them showed decreased fold change in *Bmal1*$^{-/-}$ MEFs. Pathway enrichment analysis exhibited that there were no specific pathways for Bmal1-modulated GC-responsive genes. However, other gene ontology enrichment analysis showed that Bmal1-modulated GC-responsive genes were highly related to terms, glycoprotein, oxidation-reduction, response to stimulus and extracellular region, while non-Bmal1-modulated GC-responsive genes were related to terms, intracellular, protein binding and intracellular signal transduction. Therefore, these data suggest that GR action mechanism, which is modulated by Bmal1, may be involved in several specific biological processes.

Keywords: glucocorticoid, Bmal1, microarray

INTRODUCTION

GC hormone regulates diverse physiology and behavior, including development, metabolism, inflammation, homeostasis and cognition (Biddie et al., 2012). It modulates gene expressions through the GC receptor (GR), which is bound to the multimeric complex containing hsp90, p23 and Src in the absence of GC and is released from the complex and translocates to the nucleus upon exposure to GC (Revollo and Cidlowski, 2009). Then, numerous target genes are activated or repressed according to the promoter and cellular contexts (John et al., 2008; So et al., 2007). Activated GRs directly recognize a consensus DNA sequence, GRE or nGRE to activate or repress the transcriptional activity (Kassel and Herrlich, 2007). When some of transcription factor binding sites are located in the vicinity of the GRE, the GR crosstalks with other transcription factors to positively or negatively modulate the transcriptional activity. It is also possible that tethering of GR to DNA-bound other transcription factors regulates the transcriptional activities (Kassel and Herrlich, 2007).

Bmal1 is a key transcription factor in the transcriptional and translational feedback loops of the mammalian circadian clock. It heterodimerizes with CLOCK on the E-box to turn on the transcription. Although there is not much information about the crosstalk between Bmal1 and other

transcription factors, the previous study suggested that Bmal1 differentially modulated the transcriptional activity of the GR depending on target genes (Cheon et al., 2013). Therefore, in this study, I attempted to investigate the genome-wide role of Bmal1 in the GR-mediated transcription.

MATERIALS AND METHODS

Cell culture and RNA preparation

Wild type and *Bmal1*$^{-/-}$ mouse embryonic fibroblast cells (MEFs) were prepared from day 13.5-day post coitum (dpc) and were spontaneously immortalized (Todaro and Green, 1963b). Cells were cultured in Dulbecco's s Modified Eagle Medium containing 10 % fetal bovine serum, 100 units penicillin and 100 μg/ml streptomycin at 37°C under 5 % CO_2. To prepare RNA for the microarray experiment, confluent WT and *Bmal1*$^{-/-}$MEFs were stimulated with 0.1% DMSO or 1μM DEX for 6-hr. Total RNA was extracted by TRIZOL reagent (Invitrogen) according to the manufacturer's instructions.

Microarray and statistical analysis

Microarray experiments using triplicate RNA samples were conducted at Macrogen Inc. (Seoul, Korea). After RNA purity and integrity were checked by the denaturing gel electrophoresis and the analysis of OD 260/280 ratio and OD 260/230 ratio, 550ng of total RNA was reverse-transcribed to cDNA using a T7 oligo(dT) primer. Second-strand cDNA was synthesized, in vitro transcribed and labeled with biotin-NTP using Illumina TotalPrep RNA Amplification Kit (Ambion, Austin, TX). Labeled cRNAs were hybridized to Illumina MouseRef-8 v2 Expression BeadChip (Illumina, Inc., San Diego, CA) for 16-18 hr at 58°C. Hybridized signals from

Amersham fluorolink streptavidin-Cy3 (GE Healthcare Bio-Sciences, Little Chalfont, UK) were scanned by an Illumina bead array Reader confocal scanner according to the manufacturere's instructions. Data were exported and analyzed by Illumina BeadStudio v3.1.3 (Gene Expression Module v3.3.8).

Array data were filtered by detection p-value <0.05 in more than 50% samples. Selected signal values from 11,603 probes was transformed by logarithm and normalized by quantile method. To merge signals of more than two probes for a gene, we selected one that showed maximum values of the fold change (the signal ratio of DEX-treated group versus vehicle-treated group) in WT MEFs. To examine the effect of two factors (DEX treatment and Bmal1) on gene expression, we performed 2-way analysis of variance (ANOVA) with Tuckey's HSD post-hoc test. For multiple testing corrections, each p value was adjusted by Benjamini-Hochberg false discovery rate (FDR). All data analysis was conducted in R software (version 2.4.1).

Gene clustering and gene ontology enrichment analysis

Hierarchical clustering was performed by complete linkage and Euclidean distance as a measure of similarity with normalized values by average of signals from each gene. To divide genes into several groups according to basal expression and responsiveness to DEX, we applied self

organizing tree algorithm (SOTA). Clustering analyses were conducted in MultiExperiment Viewer (MeV) 4.9.0 (http://www.tm4.org/mev.html). Pathway and gene ontology enrichment analysis were performed in the Database for Annotation, Visualization and Integrated Discovery (DAVID). The terms were selected based on FDR adjusted p-value < 10%. The analysis results of gene ontology enrichment for biological process were visualized by REVIGO (http://revigo.irb.hr/).

RESULTS

Bmal1 is a global regulator for DEX responsiveness

To examine global effects of Bmal1 on DEX responsiveness, I designed the microarray experiment using WT and *Bmal1*$^{-/-}$ MEFs after vehicle or DEX treatment. About 65% of total valid probes showed the significantly different expression level between WT and *Bmal1-/-* MEFs (Figure 16A and B). DEX treatment altered about 17% of gene expression levels, but when the cut-off value of fold change was restricted to above 1.2-fold, the expression levels of about 6% genes were significantly up- or down-regulated (Figure 16B and D). To identify the subset of genes, of which DEX responsiveness were affected by Bmal1, I analyzed the microarray data with 2-way ANOVA. The analysis results showed that 7.1% of total genes had the interaction effect between DEX treatment and Bmal1, because the expression levels of about 83% genes were not changed by DEX treatment (Figure 16C). Therefore, when the portion of genes that have the interaction effect between DEX treatment and Bmal1 in DEX responsive genes was calculated, it was increased to 57.7%, suggesting that many DEX responsive genes were regulated by Bmal1 in the activation of GC signaling pathway (Figure 17D).

When DEX responsive genes were separately analyzed depending on the direction of DEX responsiveness, the proportion of genes that showed the interaction effect between DEX treatment and Bmal1 was different

(Figure 18A). In up-regulated genes by DEX treatment, about 65% genes showed the interaction effect, but in down-regulated genes by DEX treatment, about 49% genes did. The sub-categorization depending on the degree of the fold change exhibited that genes, which showed higher fold change, were more affected by Bmal1 than those that showed lower fold change (Figure 17B).

Global interaction patterns of Bmal1 on DEX responsive genes

To scrutinize the effects of Bmal1 on DEX responsiveness, I categorized DEX responsive genes into 4 groups, which are up-regulated genes that show the interaction effect, up-regulated genes that do not show the interaction effect, down-regulated genes that show interaction effect and down-regulated genes that do not show the interaction effect. Then, each group was sub-classified into 11 clusters using the self organizing tree algorithm (SOTA).

Hierarchical clustering of up-regulated genes that show the interaction effect exhibited that DEX responsiveness was decreased in most of those genes (Figure 18A). Sub-classification by SOTA generated 11 types of gene expression patterns (Figure 18B-C and Table 1). Only about 10% of genes that belonged to clusters IU C,D and F showed similar patterns of DEX responsiveness in WT and *Bmal1*$^{-/-}$ MEFs. A common feature in these genes was that the basal expression level in vehicle-treated group of

Bmal1$^{-/-}$ MEFs was elevated or maintained (Figure 18C). However, other genes, which occupied about 90% and belonged to clusters IU A-B,E,G-K, had decreased or similar basal expression level and decreased DEX responsiveness in *Bmal1*$^{-/-}$ MEFs. Interestingly, up-regulated genes that do not show the interaction effect had different expression patterns. As the result of the statistical analysis presents, those genes exhibited similar DEX responsiveness in *Bmal1*$^{-/-}$ MEFs (Figure 19A). However, about 27% of those genes had slightly decreased basal expression level and most of them had similar or increased basal expression level in vehicle-treated group of *Bmal1*$^{-/-}$ MEFs (Figure 19B-C and Table 2). The patterns of down-regulated genes were similar to those of up-regulated genes. The basal expression level of *Bmal1*$^{-/-}$ MEFs was decreased in about 83% of the down-regulated genes that have the interaction effect. Sub-classification by SOTA showed that almost all of them except those of clusters ID I-J lost the repression ability (Figure 20A-C and Table 3). In contrast, only about 23% of the down-regulated genes that do not have the interaction effect showed decreased basal expression level in *Bmal1*$^{-/-}$ MEFs (Figure 21A-C and Table 4).

Gene ontology enrichment analysis with genes that have the interaction effect

To examine the role of the interaction effect between Bmal1 and DEX

responsiveness, I performed the gene ontology annotation enrichment analysis with the list of genes that have the interaction. Those genes were highly involved in pathways in cancer and MAPK signaling pathway (Table 5). But, the pathways were also enriched in genes that do not have the interaction effect, suggesting that genes that show the interaction effect were not related to specific signaling pathways. The results from Swit Prot (SP)-Protein Information Resource (PIR) keyword returned several functional keywords in related to the gene list (Table 6). The term phosphoprotein was enriched irrespective of whether genes have the interaction effect or not. An interesting point was that many other keywords were suggested for genes that show the interaction effect. Those genes were highly related to glycoprotein, signal, disulfide bond, secreted, oxidoreductase, iron *etc*. The cellular distributions of genes were distinctly different between two groups (Table 7). Whereas many genes that do not have the interaction effect were located in the cytoplasm, the extracellular region was suggested as the enriched site for genes that have the interaction effect. In terms of molecular function, many genes that have the interaction effect showed oxidoreductase activities and iron ion binding, while genes that do not have interaction effect were related to protein binding and transcription factor activity (Table 8). The gene ontology enrichment analysis regarding biological process indicated that most of DEX responsive genes were related to many types of developmental

process (Figure 22A and B). A distinctive feature was that genes that have the interaction effect were enriched in response pathway to the external stimuli and oxidation-reduction process.

Figure 16. Global effects of Bmal1 on DEX responsiveness. (A) Hierarchical clustering of gene expression of total probes were performed and the corresponding heat map was generated by the rainbow color scheme. Red represent high level expression and blue represent low level expression. Each group data were represented in parallel triplicate samples. (B) Venn diagram was generated using significant genes, which have adjusted *p*-value<0.05, after 2-way ANOVA with two variables (DEX treatment and Bmal1). Interaction means a complex effect of DEX treatment and Bmal1. (C) Pie graph represents what is the percentage of genes that show the interaction effect among total genes. (D) The pie graph represents what is the percentage of genes that show the interaction effect only in DEX responsive genes, which exhibit >1.2-fold change.

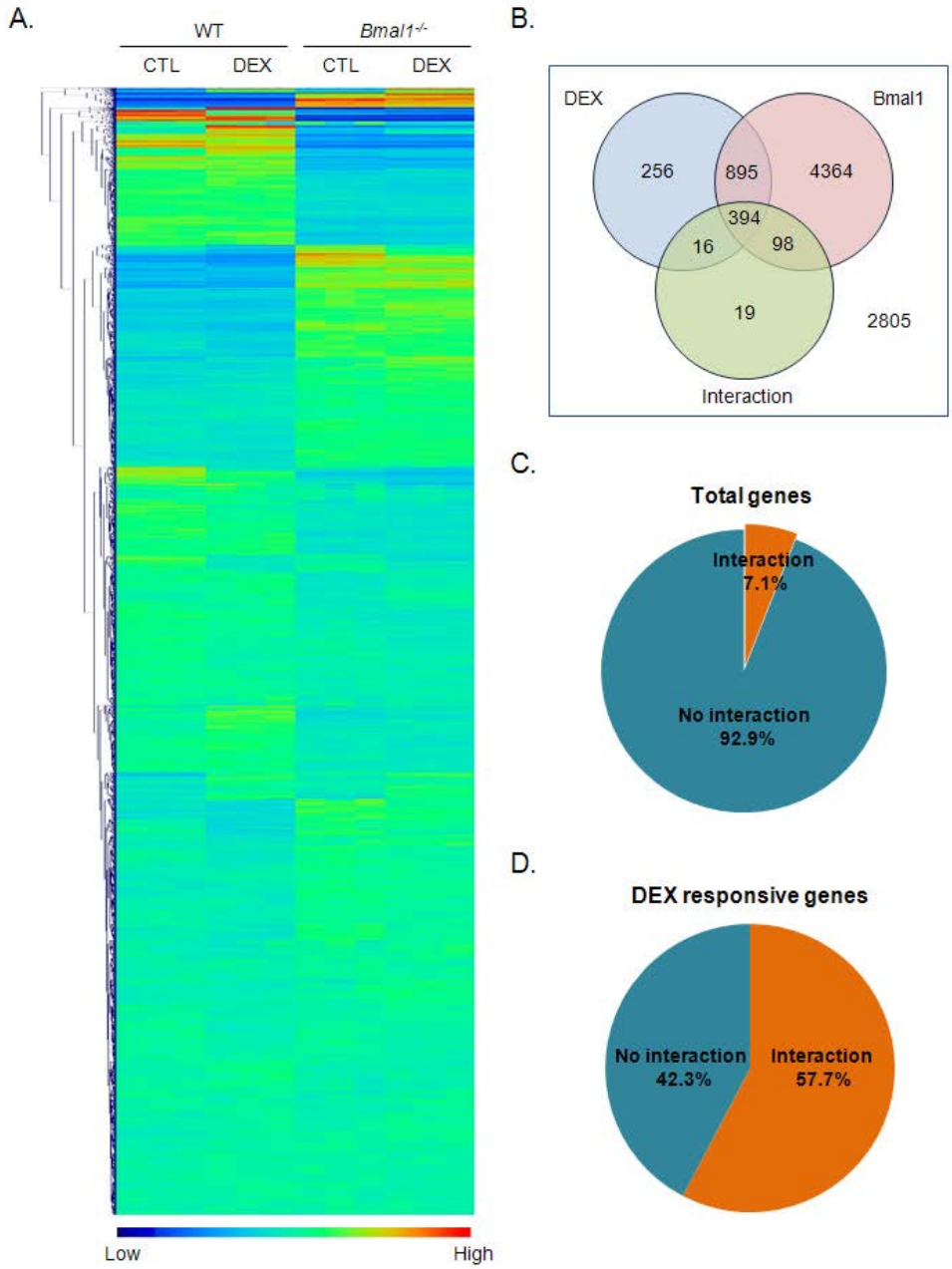
A.
WT
Bmal1-/-
CTL
DEX
CTL
DEX
Low
High
B.
DEX
Bmal1
256
895
4364
394
16
98
19
2805
Interaction
C.
Total genes
Interaction
7.1%
No interaction
92.9%
D.
DEX responsive genes
No interaction
42.3%
Interaction
57.7%

Figure 17. Gene sets that show the interaction effect between DEX treatment and Bmal1 among DEX responsive genes. (A) Up-regulated (Up) or down-regulated (down) genes by DEX treatment were divided into two groups based on the interaction effect. Red color represents genes that show the interaction and blue color represents genes that do not show the interaction. Each group was subdivided according to the degree of the fold change. Brighter color means lower fold change. (B) Up-regulated (left) or down-regulated (right) genes were divided depending on the fold change. The percentage of genes that show the interaction was represented as the blue colored bar.

A.

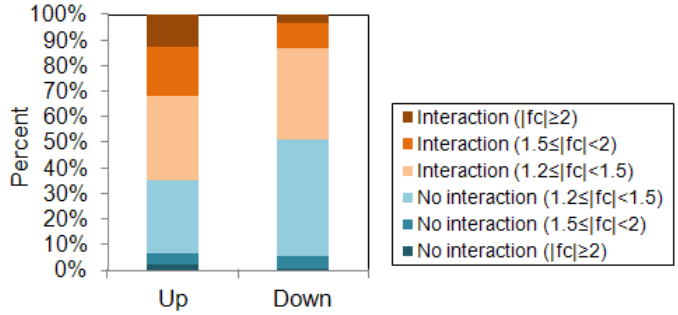
100%
90%
80%
70%
60%
50%
40%
30%
20%
10%
0%
Percent
Up
Down
Interaction (|fc|≥2)
Interaction (1.5≤|fc|<2)
Interaction (1.2≤|fc|<1.5)
No interaction (1.2≤|fc|<1.5)
No interaction (1.5≤|fc|<2)
No interaction (|fc|≥2)

B.

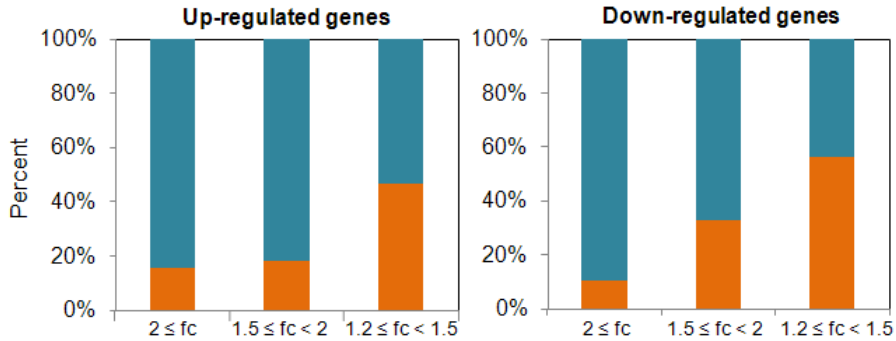
Up-regulated genes
Down-regulated genes
100%
80%
60%
40%
20%
0%
Percent
2 ≤ fc
1.5 ≤ fc < 2
1.2 ≤ fc < 1.5

Figure 18. Up-regulated genes that show the interaction effect between DEX treatment and Bmal1. (A) Among up-regulated genes by DEX treatment, 197 genes showed the interaction between DEX treatment and Bmal1. Those were clustered by the hierarchical clustering. (B) To categorize gene expression patterns, self organizing tree algorithm (SOTA) was applied for selected genes. Mean value of expression levels for each cluster was represented and hierarchical clustering was performed. (C) Expression graph for clusters (IU A~K) generated in (B). Each dot in the top and bottom line represents each sample. Expression levels of twelve samples including Triplicates for 4 experimental groups were connected by the line.

A.

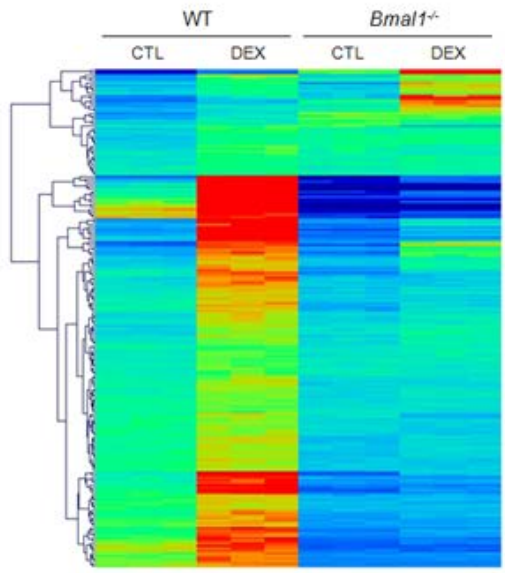
WT
Bmal1-/-
CTL
DEX
CTL
DEX

B.

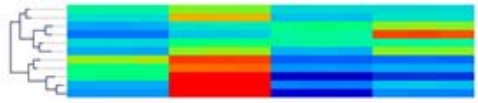

C.

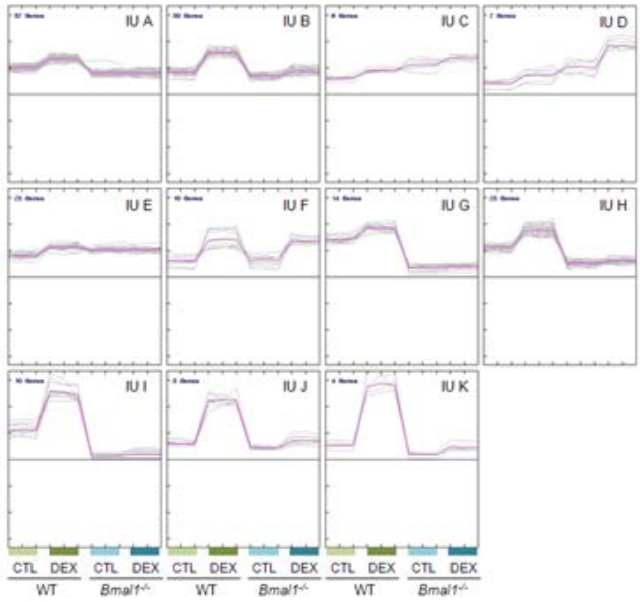
IU A
IU B
IU C
IU D
IU E
IU F
IU G
IU H
IU I
IU J
IU K
CTL DEX CTL DEX CTL DEX CTL DEX CTL DEX CTL DEX
WT Bmal1-/- WT Bmal1-/- WT Bmal1-/-

Figure 19. Up-regulated genes that do not show the interaction effect between DEX treatment and Bmal1. (A) Among up-regulated genes by DEX treatment, 107 genes did not show the interaction between DEX treatment and Bmal1. Those were clustered by the hierarchical clustering. (B) To categorize gene expression patterns, SOTA was applied for selected genes. Mean value of expression levels for each cluster was represented and hierarchical clustering was performed. (C) Expression graph for clusters (NU A~K) generated in (B). Each dot in the top and bottom line represents each sample. Expression levels of twelve samples including Triplicates for 4 experimental groups were connected by the line.

A.

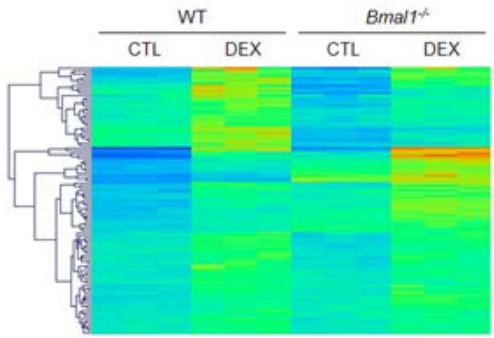
WT
Bmal1-/-
CTL
DEX
CTL
DEX

B.

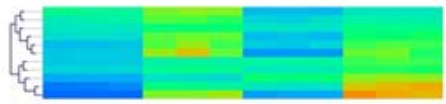

C.

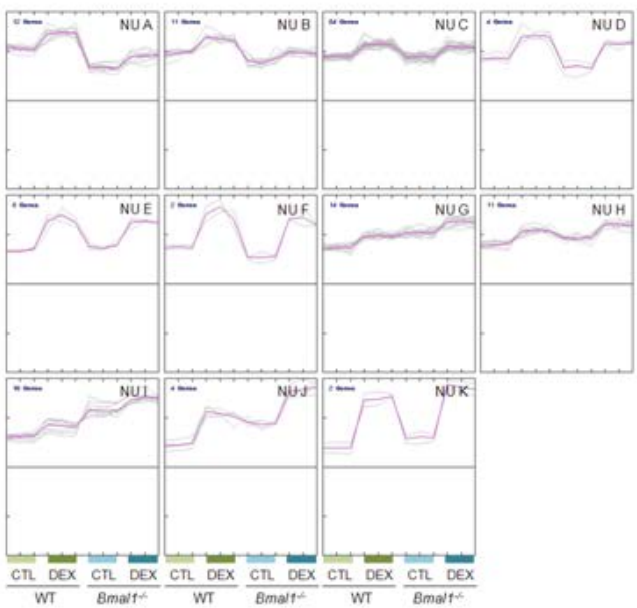
NUA
NUB
NUC
NUD
NUE
NUF
NUG
NUH
NUI
NUJ
NUK
CTL
DEX
CTL
DEX
CTL
DEX
CTL
DEX
CTL
DEX
CTL
DEX
WT
Bmal1-/-
WT
Bmal1-/-
WT
Bmal1-/-

Figure 20. Down-regulated genes that show the interaction effect between DEX treatment and Bmal1. (A) Among down-regulated genes by DEX treatment, 124 genes show the interaction between DEX treatment and Bmal1. Those were clustered by the hierarchical clustering. (B) To categorize gene expression patterns, SOTA was applied for selected genes. Mean value of expression levels for each cluster was represented and hierarchical clustering was performed. (C) Expression graph for clusters (ID A~K) generated in (B). Each dot in the top and bottom line represents each sample. Expression levels of twelve samples including Triplicates for 4 experimental groups were connected by the line.

A.

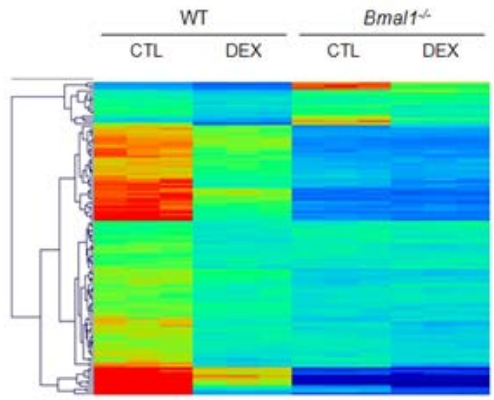
WT
Bmal1-/-
CTL
DEX
CTL
DEX

B.

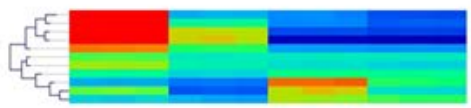

C.

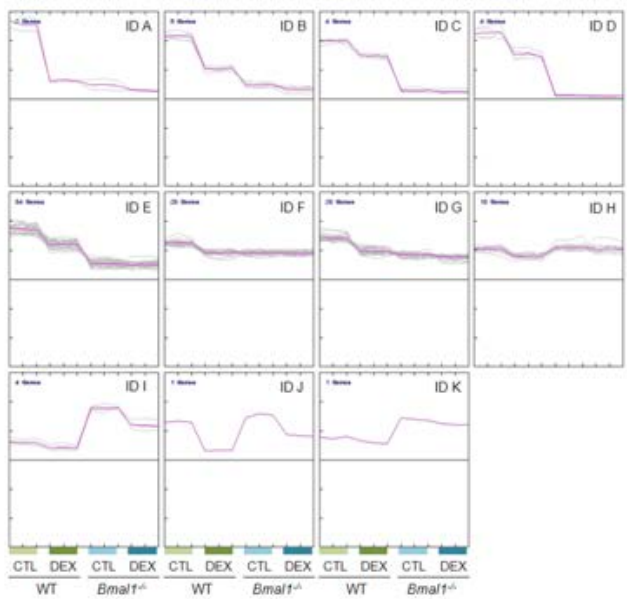
ID A
ID B
ID C
ID D
ID E
ID F
ID G
ID H
ID I
ID J
ID K
CTL DEX CTL DEX CTL DEX CTL DEX CTL DEX CTL DEX
WT
Bmal1-/-
WT
Bmal1-/-
WT
Bmal1-/-

Figure 21. Down-regulated genes that do not show the interaction effect between DEX treatment and Bmal1. (A) Among down-regulated genes by DEX treatment, 115 genes do not show the interaction between DEX treatment and Bmal1. Those were clustered by the hierarchical clustering. (B) To categorize gene expression patterns, SOTA was applied for selected genes. Mean value of expression levels for each cluster was represented and hierarchical clustering was performed. (C) Expression graph for clusters (ND A~K) generated in (B). Each dot in the top and bottom line represents each sample. Expression levels of twelve samples including Triplicates for 4 experimental groups were connected by the line.

A.

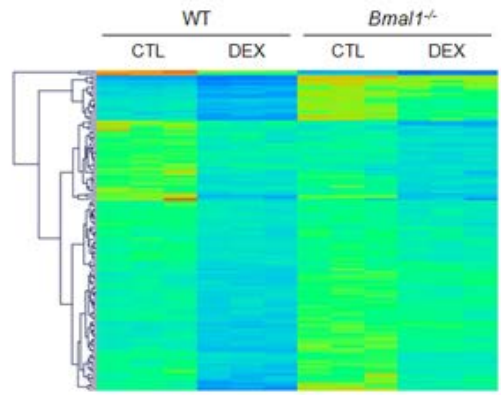
WT
Bmal1-/-
CTL
DEX
CTL
DEX

B.

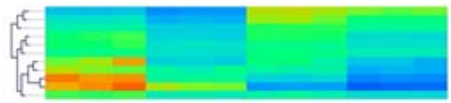

C.

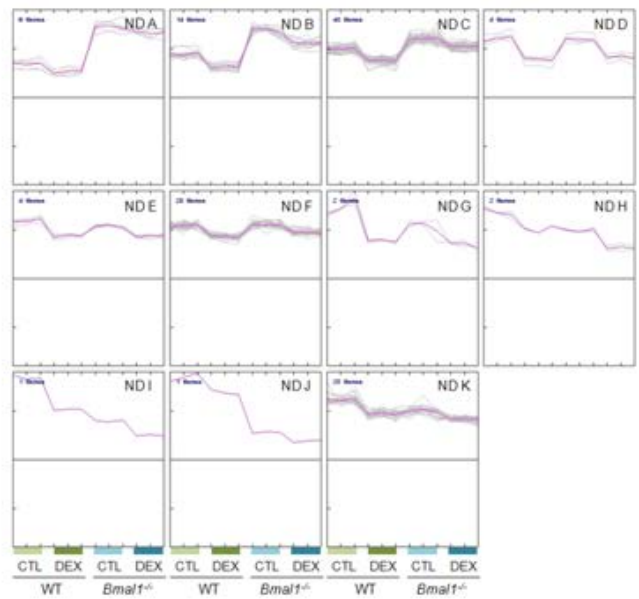
NDA
NDB
NDC
NDD
NDE
NDF
NDG
NDH
NDI
NDJ
NDK
CTL
DEX
CTL
DEX
CTL
DEX
CTL
DEX
CTL
DEX
WT
Bmal1-/-
WT
Bmal1-/-
WT
Bmal1-/-

Figure 22. Gene ontology enrichment analysis for biological processes. Gene ontology enrichment was analyzed for genes that have the interaction (A) and genes that do not have the interaction (B). Gene ontology terms were visualized according to *p*-value and the generality of the gene ontology term. The bubble size indicates the generality of the term and the bubble color indicates the adjusted *p*-value. Highly similar terms are linked by edges and the line width indicates the degree of similarity.

A.

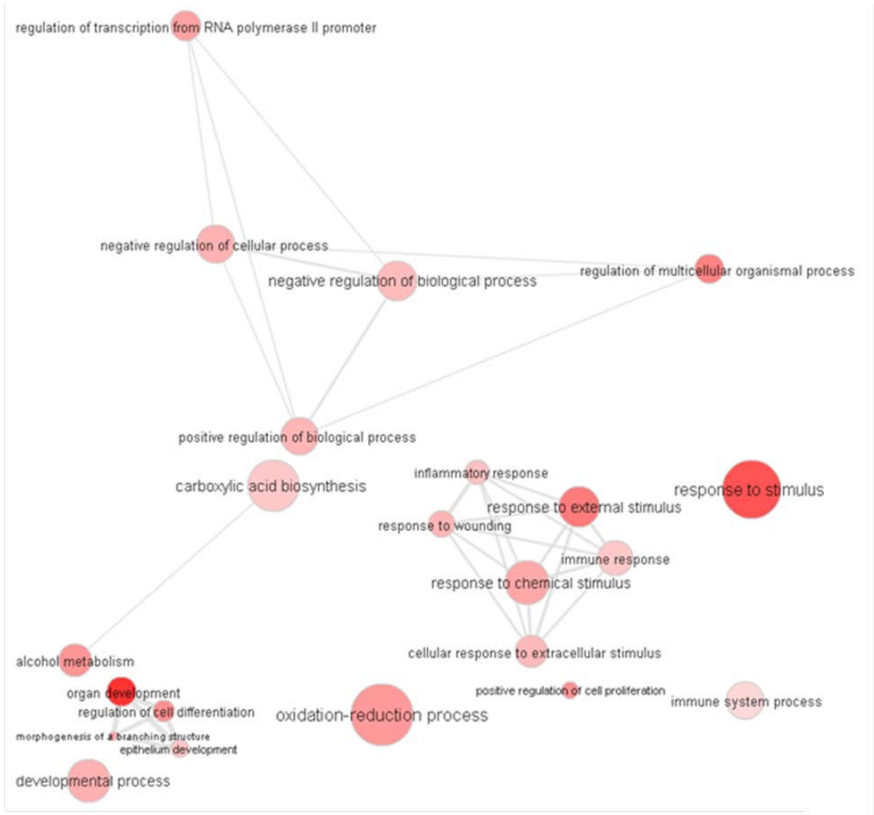
regulation of transcription from RNA polymerase II promoter
negative regulation of cellular process
negative regulation of biological process
regulation of multicellular organismal process
positive regulation of biological process
carboxylic acid biosynthesis
inflammatory response
response to stimulus
response to external stimulus
response to wounding
immune response
response to chemical stimulus
cellular response to extracellular stimulus
alcohol metabolism
organ development
regulation of cell differentiation
morphogenesis of a branching structure
epithelium development
oxidation-reduction process
positive regulation of cell proliferation
immune system process
developmental process

B.

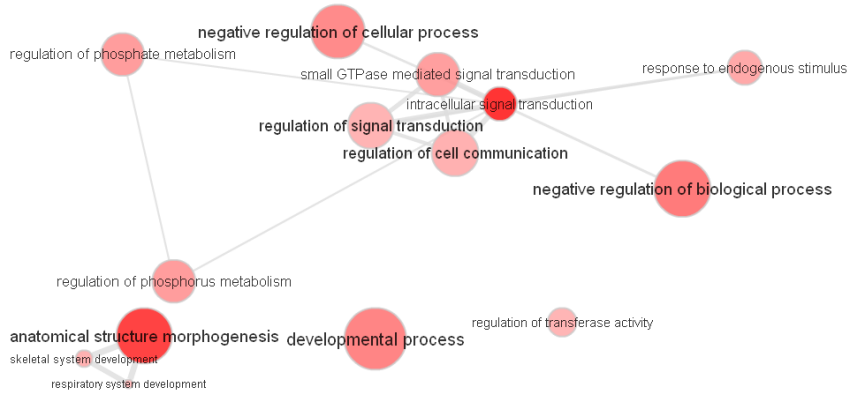
negative regulation of cellular process
regulation of phosphate metabolism
small GTPase mediated signal transduction
response to endogenous stimulus
intracellular signal transduction
regulation of signal transduction
regulation of cell communication
negative regulation of biological process
regulation of phosphorus metabolism
anatomical structure morphogenesis
developmental process
regulation of transferase activity
skeletal system development
respiratory system development

Table 1. Classification of up-regulated genes that show the interaction effect between DEX treatment and Bmal1 by SOTA.

IU A		IU B	IU C	IU D	IU E
Gadd45g	Fads3	1190002H23Rik	Aldh4a1	Smpd3	Mertk
Plekhf1	Grasp	Per2	Man2b1	Pdk4	Suox
Fam129b	Jtv1	Map3k6	Mmp2	LOC100038894	Sidt2
Bcat2	Abhd2	Mocs1	1810011O10Rik	Klra4	Nuak2
Anxa8	Dag1	Anxa1	H6pd	Ly6c1	D16H22S680E
Snx10	Tpst2	Klf13	Sdpr	Sesn1	1110008P14Rik
Igsf3	Aldh3a1	Myocd		Kcnj15	BC099439
LOC435337	Bcl6	Vdr			Efnb1
Zfp36	Hipk3	Glrx			OTTMUSG00000025408
Col15a1	Rassf7	Pias1			Eef2k
Llgla2	Mfsd7a	1700088E04Rik			Dtnb
LOC100045551	P2ry6	Tead4			Ddx28
Fhl2	Otud7b	Chrd			Flot2
Irak3	Htra2	Als2cr13			4931408A02Rik
Adck4	Il13ra1	Klf2			Sav1
Gdpd2	Tfrc	Rilpl1			Spen
Lamc2	Gprc5a	Piga			Ass1
2310016C08Rik	D5Wsu178e	Tob2			Atg12
Slc39a14	Sprr2k	Chst8			Socs2
Cenpm	Jun	Tbl2			Mgll
Oxsr1	C1qtnf1	Rhoj			Sdc4
Psca	Plxna2	Axud1			Ankzf1
Hdac7	Zfp185	B4galt1			Fkhl18
Gfpt2	Me2	Akr1b3			
Srm	Jmjd6	Adra2a			
Nedd9	Grk5	Porcn			
Ihpk2	Ldha	Ppyr1			
Ogfod1		Ppm2c			
Nbl1		Irs2			
Ap2a2		Peli2			

IU F	IU G	IU H	IU I	IU J	IU K
Errfi1	Calml4	Figf	Scara5	Cyb561	Serpina3n
Fkbp5	Tmem119	Klf5	Gas6	Slc10a6	Dlk2
Notch4	Serpina3g	Fos	Ppl	Crispld2	Mt2
LOC100046232	Steap2	Atp10d	Serpina3h	Lims2	9130213B05Rik
4930486L24Rik	Kng1	6330406I15Rik	Lcn2	Slc6a12	
Gldc	Apcdd1	Gcnt2	Xdh	Sepp1	
2900062L11Rik	Vegfc	Dusp1	Cyp2d22	Tmem38b	
Per1	Smoc1	Il1rl1	Saa3	Hspb1	
Sgk1	Eno2	A530050D06Rik	Tgm2		
Serpina3f	Prickle1	Lbp	Plac8		
	Ndrl	Pla1a			
	Slc2a3	1190007F08Rik			
	Pdgfra	Scd1			
	Apobec1	E2f6			
		Egln3			
		Prss23			
		Map3k8			
		1700025G04Rik			
		Rrp12			
		Rora			
		Cdkn1c			
		Ifitm2			
		Pgam1			
		Slco3a1			
		Slc2a1			
		LOC100047934			
		Kctd10			
		Gm129			

Table 2. Classification of up-regulated genes that do not show the interaction effect between DEX treatment and Bmal1 by SOTA.

NUA	NUB	NUC		NUD	NUE
Epn2	Clec2d	Cltb	Slc31a2	Klf9	Foxred2
Ndufb6	Bex2	Exosc6	Spc24	Rras2	Rhob
Vldlr	Polr2f	Ipmk	Podxl	Samhd1	Usp2
Elovl5	LOC100044177	Rev3l	Sh3gl1	Depdc6	
Hsp105	Snai1	Rnf125	Myadm		
Slc6a6	Hip1r	LOC100046457	6430548M08Rik		
Ly6a	B230342M21Rik	Snx1	Mef2b		
Por	Bcl2l1	Fbxo2	Stim1		
Pim3	Tmem167	Itga3	Tha1		
Pscd3	2310022B05Rik	Ralb	Vamp2		
Ep300	Letm1	Slc25a17	Sorbs3		
1110059E24Rik		Dcbld2	Nek9		
		Dtx4	Fndc3b		
		Irf2	D19Wsu162e		
		9330176C04Rik	Bnip3l		
		Stk24	BC043301		
		S100a10	Fam169b		

NUF	NUG	NUH	NUI	NUJ	NUK
Adamts1	Gprc5b	S3-12	Mcf2l	Cdo1	Tsc22d3
4930572J05Rik	Podxl2	Slc7a6	Gpr64	Hp	Snta1
	Mknk2	Pik3r1	Lox	Spsb1	
	Tm2d2	Plce1	Rhou	Pla2g15	
	D8Ertd82e	Smarcd2	LOC100047261		
	Helb	Zhx3	Moxd1		
	Lrrc8	Ehd4	Fhl1		
	Tbc1d2b	Lrrc8a	BC031353		
	Cdkn1a	Sec63	St6gal1		
	Arl4a	Sept9	Insl6		
	Inpp5k	Zfp1			
	Ids				
	Hps3				
	P4ha1				

Table 3. Classification of down-regulated genes that show the interaction effect between DEX treatment and Bmal1 by SOTA.

ID A	ID B	ID C	ID D	ID E	
Cxcl1	LOC100047427	Pdlim4	Mfap5	Enpp2	Hspa12b
Ch25h	Bach2	Sfrp1	Cyp7b1	Dennd3	Ugcg
	Vcam1	Pde1b	Rasl11a	Ldb2	Gpr176
	Ednra	Angptl4	Ccl7	Hoxb6	Cd14
	D0H4S114			Elovl6	Aoc3
				Cbx7	Il7
				Gp38	Gbp2
				Hsd17b7	5430435G22Rik
				Arrdc4	1200002N14Rik
				Twist2	Gbp3
				Slit2	Fas
				Hoxb5	Shox2
				Plscr1	Rbm47
				Soat2	Rgs16
				D4Bwg0951e	Oasl2
				Hoxc10	Dbp
				Pftk1	Tlr2

ID F	ID G	ID H	ID I	ID J	ID K
Tctex1d2	Plscr4	Kctd5	Inhba	Phlda1	Pi4k2b
Cdr2	Gclm	Tcirg1	Slc40a1		
Mrps6	Slc6a9	Ttc26	Cdsn		
Nfkbil2	LOC100040592	Aqp3	Ank		
Ttc7	Twist1	Manea			
Hic1	Gcnt1	Gnptab			
Agrn	Mogat2	Trib2			
Lrp12	Osr2	LOC100044736			
Rab32	Sod2	Hs6st1			
Mycl1	Slc27a6	Gpr23			
Podn	Ltbp2	Ube1l			
Ermp1	Clip4	Tle6			
Ttyh3	Arhgap18	Amigo2			
Rsn	Rai14				
Psmb9	Slc6a17				
Sc4mol	Garnl4				
Chst2	Adamts4				
Tgfb1	Nfkbie				
Plaur	Nope				
Grem1	Cxcl16				
D12Ertd553e	Zfpm2				
Stbd1	Lhfpl2				
OTTMUSG00000004461	Micall2				
Gypc	Fzd7				
Mcc	Pdlim3				
Tmem86a	Plk2				
Ttyh2	Fgf7				
Npy1r	Relb				

Table 4. Classification of down-regulated genes that do not show the interaction effect between DEX treatment and Bmal1 by SOTA.

ND A	ND B	ND C		ND D	ND E
Dyrk1b	Rassf5	Pigx	Tnfaip8	Egr2	Etv5
Ttc5	Hgf	Coro2b	Sertad4	Man2a1	Lbh
Mmp14	C79267	Dfna5h	Gpr153	Meox1	Rasa1
Arhgef4	Vangl2	Cirbp	Fgfrl1	Gadd45a	Traf3
Slc1a3	Osbpl3	Samd14	LOC100046883		
Endod1	Fchsd1	H3f3b	Rrad		
	Pik3r3	Ercc2	Pdlim7		
	Ank1	Cklf	Zeb1		
	Ly96	Zswim4	Tulp4		
	Prmt2	6430510M02Rik	Samd9l		
	Tgfb3	Spsb2	Map2k6		
	Igtp	1200014J11Rik	3110050N22Rik		
	Pkia	Zmym3	Ddit3		
	Igsf9	Mboat1	Pja2		
		Vat1	Hoxb2		
		Tiam2	Smad3		
		LOC100047480	Tsc22d2		
		Palld	Tle2		
		Stat1	Rapgef6		
		Fbn1	Has2		
		Ccdc120	Gab1		
		Leprotl1			

ND F	ND G	ND H	ND I	ND J	ND K
Mapk11	Hes1	Cxadr	Wisp1	Pdzrn3	Cdk5rap2
6720460F02Rik	Usp18	Prkg2			Brunol4
Rras					Itpr1
2310003H01Rik					C1rl
Upp1					Gnpda2
Nrn1					Pdgfrb
2610020C11Rik					Npr3
Raet1b					Arhgef2
Pou6f1					Scmh1
Nfkb1					Areg
Psmb10					Lif
Trim21					Etv4
Cstad					Ak5
Tsga14					Mical2
Pigp					Schip1
Tead2					D230007K08Rik
5330401P04Rik					Il10rb
2610208M17Rik					Parp14
Tspan2					LOC100048346
Mov10					Ptn
Cd44					Apol9b
Rgs12					Pea15
Camk2n1					Iqgap1
1110012J17Rik					
Ankrd50					
Dusp8					
Mex3a					
Hbegf					

Table 5. Results from the pathway enrichment analysis.

Pathway	Count	%	P value	FDR
Interaction				
mmu05200:Pathways in cancer	14	4.745763	0.00906	9.8662577
mmu04010:MAPK signaling pathway	13	4.40678	0.00488	5.4232279
No interaction				
mmu05200:Pathways in cancer	15	6.9124424	$5.92X10^{-5}$	0.0647058
mmu04010:MAPK signaling pathway	12	5.5299539	$5.82X10^{-4}$	0.6343927
mmu04810:Regulation of actin cytoskeleton	10	4.6082949	0.0019185	2.0760618
mmu05212:Pancreatic cancer	8	3.6866359	$3.67X10^{-5}$	0.0400471
mmu04620:Toll-like receptor signaling pathway	8	3.6866359	$2.80X10^{-4}$	0.3051496
mmu05220:Chronic myeloid leukemia	7	3.2258065	$4.32X10^{-4}$	0.4705406
mmu05211:Renal cell carcinoma	6	2.764977	0.0020838	2.2531048
mmu05222:Small cell lung cancer	6	2.764977	0.0048537	5.1766567
mmu04012:ErbB signaling pathway	6	2.764977	0.0053584	5.7007334
mmu05215:Prostate cancer	6	2.764977	0.0061837	6.5520248

Table 6. Results from SP-PIR keywords enrichment analysis.

Term	Count	%	P value	FDR
Interaction				
phosphoprotein	124	42.0339	0.00313	4.066284
glycoprotein	99	33.55932	$9.40X10^{-9}$	$1.24X10^{-5}$
signal	68	23.05085	0.001494	1.961211
disulfide bond	65	22.0339	$4.19X10^{-5}$	0.05546
Secreted	42	14.23729	$1.44X10^{-4}$	0.189959
oxidoreductase	22	7.457627	$3.42X10^{-4}$	0.452365
Signal-anchor	16	5.423729	0.002208	2.884953
iron	15	5.084746	$6.60X10^{-4}$	0.870137
lipid synthesis	9	3.050847	$1.82X10^{-4}$	0.240726
LIM domain	7	2.372881	0.001071	1.409762
Proto-oncogene	7	2.372881	0.002493	3.252068
No interaction				
phosphoprotein	97	44.70046	$1.83X10^{-4}$	0.23669
cytoplasm	50	23.04147	0.004485	5.644667

Table 7. Results from the cellular component ontology enrichment analysis.

Term	Count	%	P value	FDR
Interaction				
GO:0005576~extracellular region	45	15.25424	5.05E-04	0.642071
GO:0044421~extracellular region part	28	9.491525	9.42E-05	0.120042
GO:0005615~extracellular space	20	6.779661	4.93E-04	0.627395
GO:0005829~cytosol	18	6.101695	0.006366	7.824243
GO:0031012~extracellular matrix	13	4.40678	0.003739	4.666141
GO:0005578~proteinaceous extracellular matrix	12	4.067797	0.007565	9.232705
No interaction				
GO:0005622~intracellular	131	60.36866	0.004995	6.286084
GO:0005737~cytoplasm	93	42.85714	0.002527	3.227099
GO:0044459~plasma membrane part	31	14.28571	0.005045	6.347756
GO:0000267~cell fraction	15	6.912442	0.007755	9.60185

Table 8. Results from the molecular function ontology enrichment analysis.

Term	Count	%	P value	FDR
Interaction				
GO:0016491~oxidoreductase activity	26	8.813559	3.46E-04	0.499576
GO:0005506~iron ion binding	16	5.423729	5.43E-04	0.782772
GO:0016705~oxidoreductase activity, acting on paired donors, with incorporation or reduction of molecular oxygen	9	3.050847	0.004172	5.865694
GO:0015294~solute:cation symporter activity	6	2.033898	0.006853	9.46468
No interaction				
GO:0005515~protein binding	90	41.47465	2.58E-04	0.356729
GO:0005488~binding	149	68.66359	4.17E-04	0.575765
GO:0003700~transcription factor activity	18	8.294931	0.006857	9.091952

DISCUSSION

In the present study, I found that Bmal1 affected about half of GC-responsive genes by a 2-way ANOVA analysis, the most of which lost GC responsiveness in Bmal1$^{-/-}$ MEFs. Those genes were highly related to gene ontology terms such as glycoprotein, oxidation-reduction and response to stimulus, suggesting that Bmal1-modulated GC regulation might be involved in some specific biological processes.

Previous studies reported that core clock genes affected the transcriptional regulation activity of GR. GRE-mediated transactivation could be modulated by the histone acetyltransferase activity of CLOCK, which induces the release of GR from GRE (Nader et al., 2009). Circadian repressors, Cry1 and Cry2, widely repressed GR-mediated transcriptional regulation (Lamia et al., 2011). These studies commonly proposed the core clock genes as negative regulators for the action of GR unilaterally. However, another study in my lab rendered the evidence of differential regulation of Bmal1 for the GR action according to the promoter (Cheon et al., 2013). In line with this, the present genome-wide study suggests that Bmal1 regulates GC-responsive genes in both directions. More than half of GC-responsive genes, including both up- and down-regulated genes, did not respond to DEX treatment when Bmal1 was absent.

Different regulation patterns in GC-responsive genes may derive from several possibilities. Since GR has higher affinity to the palindromic GRE

compared to the non-palindromic sequence, non-Bmal1 dependent GC-responsive genes are likely to have palindromic GREs (Scott et al., 1998). The distance between GRE and E-box is another variable for the functional interaction of Bmal1 and GR. While the GRE is overlapped with E-box by 1-bp in Bmal1-modulated GC-responsive gene, Per2, five E-boxes locate away from the GRE in Per1 that can be induced by DEX in Bmal1$^{-/-}$ MEFs. Even in Per2 promoter, the GRE functionally interacts with the overlapped E-box, rather than distant E-box (Cheon et al., 2013). Considering previous ChIP-seq data, there is the other possibility of the particular motif for Bmal1-modulated GC-responsive genes (Uhlenhaut et al., 2012). This motif might pre-determine the chromatin opening and the occupancy of cofactors (John et al., 2011; Reddy et al., 2012; Uhlenhaut et al., 2012).

Gene ontology enrichment analysis results exhibited that several terms regarding biological processes and functions were differentially abundant according to whether genes have the interaction effect between Bmal1 and DEX treatment or not (Figure 22 and Table 5-8). Although the present study could not examine all genes due to the invalid microarray signals, the results suggested that the functional interaction with Bmal1 of GC-responsive genes was involved in response to the external stimuli. Contrary to this relationship, non-Bmal1-modulated GC-responsive genes were related to the endogenous stimuli (Figure 22). Because PAS family members are considered to be sensors of environmental and

developmental signals, it is plausible for Bmal1, or CLOCK:BMAL1 heterodimer, to act as a sensor for the timed regulation or other external stimuli (Gu et al., 2000). The terms glycoprotein and oxidoreductase activity were also related to Bmal1-modulated GC-responsive genes, implying some possibility that those biological processes result from the recognition of environmental changes (Figure 22, Table6 and 8).

The present study revealed that the global regulatory patterns of GC-responsive genes were affected by Bmal1 in MEFs. The proportion of Bmal1-modulated GC-responsive genes was more than expected, suggesting that we have to consider this mechanism in general for studying GC actions. Particularly, further studies, with respect to several enriched gene ontology terms regarding to Bmal1-modulated GC-responsive genes, could open new windows for GC regulation pathways.

REFERENCES

Akashi, M., Ichise, T., Mamine, T., and Takumi, T. (2006) Molecular mechanism of cell-autonomous circadian gene expression of Period2, a crucial regulator of the mammalian circadian clock. Mol Biol Cell *17*, 555-565.

Albrecht, U. (2012) Timing to perfection: the biology of central and peripheral circadian clocks. Neuron *74*, 246-260.

Albrecht, U., Zheng, B., Larkin, D., Sun, Z.S., and Lee, C.C. (2001) mPer1 and mPer2 are essential for normal resetting of the circadian clock. J Biol Rhythms *16*, 100-104.

Bae, K., Jin, X., Maywood, E.S., Hastings, M.H., Reppert, S.M., and Weaver, D.R. (2001) Differential functions of mPer1, mPer2, and mPer3 in the SCN circadian clock. Neuron *30*, 525-536.

Bae, K., and Weaver, D.R. (2003) Light-induced phase shifts in mice lacking mPER1 or mPER2. J Biol Rhythms *18*, 123-133.

Balsalobre, A., Brown, S.A., Marcacci, L., Tronche, F., Kellendonk, C., Reichardt, H.M., Schütz, G., and Schibler, U. (2000a) Resetting of circadian time in peripheral tissues by glucocorticoid signaling. Science *289*, 2344-2347.

Balsalobre, A., Damiola, F., and Schibler, U. (1998) A serum shock induces circadian gene expression in mammalian tissue culture cells. Cell *93*, 929-937.

Balsalobre, A., Marcacci, L., and Schibler, U. (2000b) Multiple signaling pathways elicit circadian gene expression in cultured Rat-1 fibroblasts. Curr Biol *10*, 1291-1294.

Barclay, J.L., Husse, J., Bode, B., Naujokat, N., Meyer-Kovac, J., Schmid, S.M., Lehnert, H., and Oster, H. (2012) Circadian desynchrony promotes metabolic disruption in a mouse model of shiftwork. PLoS One *7*, e37150.

Bellet, M.M., and Sassone-Corsi, P. (2010) Mammalian circadian clock and metabolism–the epigenetic link. J Cell Sci *123*, 3837-3848.

Biddie, S.C., Conway-Campbell, B.L., and Lightman, S.L. (2012) Dynamic regulation of glucocorticoid signalling in health and disease. Rheumatology *51*, 403-412.

Bunger, M.K., Wilsbacher, L.D., Moran, S.M., Clendenin, C., Radcliffe, L.A., Hogenesch, J.B., Simon, M.C., Takahashi, J.S., and Bradfield, C.A. (2000) Mop3 Is an Essential Component of the Master Circadian Pacemaker in Mammals. Cell *103*, 1009-1017.

Calomme, C., Dekoninck, A., Nizet, S., Adam, E., Nguyên, T.L.A., Van Den Broeke, A., Willems, L., Kettmann, R., Burny, A., and Van Lint, C. (2004) Overlapping CRE and E box motifs in the enhancer sequences of the bovine leukemia virus 5′ long terminal repeat are critical for basal and acetylation-dependent transcriptional activity of the viral promoter: implications for viral latency. J Virol *78*, 13848-13864.

Carpen, J.D., Archer, S.N., Skene, D.J., Smits, M., and Schantz, M. (2005) A single-nucleotide polymorphism in the 5′-untranslated region of the hPER2 gene is associated with diurnal preference. J Sleep Res *14*, 293-297.

Cermakian, N., Lamont, E.W., Boudreau, P., and Boivin, D.B. (2011) Circadian clock gene expression in brain regions of Alzheimer's disease patients and control subjects. J Biol Rhythms *26*, 160-170.

Cermakian, N., Monaco, L., Pando, M.P., Dierich, A., and Sassone-Corsi, P. (2001) Altered behavioral rhythms and clock gene expression in mice with a targeted mutation in the Period1 gene. EMBO J *20*, 3967-3974.

Chen, R., Schirmer, A., Lee, Y., Lee, H., Kumar, V., Yoo, S.H., Takahashi, J.S., and Lee, C. (2009) Rhythmic PER abundance defines a critical nodal point for negative feedback within the circadian clock mechanism. Mol Cell *36*, 417-430.

Cheon, S., Park, N., Cho, S., and Kim, K. (2013) Glucocorticoid-mediated Period2 induction delays the phase of circadian rhythm. Nucleic Acids Res.

Cho, K., Ennaceur, A., Cole, J.C., and Suh, C.K. (2000) Chronic jet lag produces cognitive deficits. J Neurosci *20*, 1-5.

Chung, S., Son, G.H., and Kim, K. (2011) Circadian rhythm of adrenal glucocorticoid: its regulation and clinical implications. Biochim Biophys

Acta *1812*, 581-591.

Dallmann, R., Touma, C., Palme, R., Albrecht, U., and Steinlechner, S. (2006) Impaired daily glucocorticoid rhythm in Per1 Brd mice. J Comp Physiol A Neuroethol Sens Neural Behav Physiol *192*, 769-775.

De Bacquer, D., Van Risseghem, M., Clays, E., Kittel, F., De Backer, G., and Braeckman, L. (2009) Rotating shift work and the metabolic syndrome: a prospective study. Int J Epidemiol *38*, 848-854.

Dibner, C., Schibler, U., and Albrecht, U. (2010) The mammalian circadian timing system: organization and coordination of central and peripheral clocks. Annu Rev Physiol *72*, 517-549.

Dickmeis, T. (2009) Glucocorticoids and the circadian clock. J Endocrinol *200*, 3-22.

Emery, P., So, W.V., Kaneko, M., Hall, J.C., and Rosbash, M. (1998) CRY, a Drosophila clock and light-regulated cryptochrome, is a major contributor to circadian rhythm resetting and photosensitivity. Cell *95*, 669-679.

Esquirol, Y., Bongard, V., Mabile, L., Jonnier, B., Soulat, J.M., and Perret, B. (2009) Shift work and metabolic syndrome: respective impacts of job strain, physical activity, and dietary rhythms. Chronobiol Int *26*, 544-559.

Feillet, C.A., Ripperger, J.A., Magnone, M.C., Dulloo, A., Albrecht, U., and Challet, E. (2006) Lack of Food Anticipation in Per2 Mutant Mice. Curr Biol *16*, 2016-2022.

Fonken, L.K., Workman, J.L., Walton, J.C., Weil, Z.M., Morris, J.S., Haim, A., and Nelson, R.J. (2010) Light at night increases body mass by shifting the time of food intake. Proc Natl Acad Sci U S A *107*, 18664-18669.

Gallego, M., and Virshup, D.M. (2007) Post-translational modifications regulate the ticking of the circadian clock. Nat Rev Mol Cell Biol *8*, 139-148.

Gu, Y.Z., Hogenesch, J.B., and Bradfield, C.A. (2000) The PAS superfamily: sensors of environmental and developmental signals. Annu Rev Pharmacol Toxicol *40*, 519-561.

Harrington, M. (2010) Location, location, location: important for jet-lagged circadian loops. The Journal of clinical investigation *120*, 2265-2267.

Hattori, M.-A. (2011) Hormonal Regulation of Circadian Pacemaker in Ovary and Uterus, Update on Mechanisms of Hormone Action - Focus on Metabolism, Growth and Reproduction, Prof. Gianluca Aimaretti (Ed.).

Herichova, I., Zeman, M., Stebelova, K., and Ravingerova, T. (2005). Effect of streptozotocin-induced diabetes on daily expression of per2 and dbp in the heart and liver and melatonin rhythm in the pineal gland of Wistar rat. Mol Cell Biochem *270*, 223-229.

Hirota, T., Okano, T., Kokame, K., Shirotani-Ikejima, H., Miyata, T., and Fukada, Y. (2002) Glucose Down-regulates Per1 and Per2mRNA Levels

and Induces Circadian Gene Expression in Cultured Rat-1 Fibroblasts. J Biol Chem *277*, 44244-44251.

Huang, N., Chelliah, Y., Shan, Y., Taylor, C.A., Yoo, S.H., Partch, C., Green, C.B., Zhang, H., and Takahashi, J.S. (2012) Crystal Structure of the Heterodimeric CLOCK: BMAL1 Transcriptional Activator Complex. Science *337*, 189-194.

Ishida, A., Mutoh, T., Ueyama, T., Bando, H., Masubuchi, S., Nakahara, D., Tsujimoto, G., and Okamura, H. (2005) Light activates the adrenal gland: timing of gene expression and glucocorticoid release. Cell Metab *2*, 297-307.

Izumo, M., Sato, T.R., Straume, M., and Johnson, C.H. (2006) Quantitative analyses of circadian gene expression in mammalian cell cultures. PLoS Comput Biol *2*, e136.

John, S., Sabo, P.J., Johnson, T.A., Sung, M.-H., Biddie, S.C., Lightman, S.L., Voss, T.C., Davis, S.R., Meltzer, P.S., and Stamatoyannopoulos, J.A. (2008) Interaction of the glucocorticoid receptor with the chromatin landscape. Mol Cell *29*, 611-624.

John, S., Sabo, P.J., Thurman, R.E., Sung, M.-H., Biddie, S.C., Johnson, T.A., Hager, G.L., and Stamatoyannopoulos, J.A. (2011) Chromatin accessibility pre-determines glucocorticoid receptor binding patterns. Nat Genet *43*, 264-268.

Jung, H., Choe, Y., Kim, H., Park, N., Son, G.H., Khang, I., and Kim, K. (2003) Involvement of CLOCK: BMAL1 heterodimer in serum-responsive mPer1 induction. Neuroreport *14*, 15-19.

Kassel, O., and Herrlich, P. (2007) Crosstalk between the glucocorticoid receptor and other transcription factors: molecular aspects. Mol Cell Endocrinol *275*, 13-29.

Katzenberg, D., Young, T., Finn, L., Lin, L., King, D.P., Takahashi, J.S., and Mignot, E. (1998) A CLOCK polymorphism associated with human diurnal preference. Sleep.

Kiessling, S., Eichele, G., and Oster, H. (2010) Adrenal glucocorticoids have a key role in circadian resynchronization in a mouse model of jet lag. The Journal of clinical investigation *120*, 2600.

Kolla, B.P., and AUGER, R.R. (2011) Jet lag and shift work sleep disorders: How to help reset the internal clock. Cleve Clin J Med *78*, 675-684.

Kopp, C., Albrecht, U., Zheng, B., and Tobler, I. (2002) Homeostatic sleep regulation is preserved in mPer1 and mPer2 mutant mice. Eur J Neurosci *16*, 1099-1106.

Lamia, K.A., Papp, S.J., Ruth, T.Y., Barish, G.D., Uhlenhaut, N.H., Jonker, J.W., Downes, M., and Evans, R.M. (2011) Cryptochromes mediate rhythmic repression of the glucocorticoid receptor. Nature *480*, 552-556.

Le Minh, N., Damiola, F., Tronche, F., Schütz, G., and Schibler, U. (2001)

Glucocorticoid hormones inhibit food-induced phase-shifting of peripheral circadian oscillators. EMBO J *20*, 7128-7136.

Lee, Y., Chen, R., Lee, H., and Lee, C. (2011) Stoichiometric relationship among clock proteins determines robustness of circadian rhythms. J Biol Chem *286*, 7033-7042.

Lightman, S.L., and Conway-Campbell, B.L. (2010) The crucial role of pulsatile activity of the HPA axis for continuous dynamic equilibration. Nature Rev Neurosci *11*, 710-718.

Maywood, E., Mrosovsky, N., Field, M., and Hastings, M. (1999) Rapid down-regulation of mammalian period genes during behavioral resetting of the circadian clock. Proc Natl Acad Sci U S A *96*, 15211-15216.

Meijsing, S.H., Pufall, M.A., So, A.Y., Bates, D.L., Chen, L., and Yamamoto, K.R. (2009) DNA binding site sequence directs glucocorticoid receptor structure and activity. Science *324*, 407-410.

Mikuni, S., Tamura, M., and Kinjo, M. (2007) Analysis of intranuclear binding process of glucocorticoid receptor using fluorescence correlation spectroscopy. FEBS Lett *581*, 389-393.

Mishima, K., Tozawa, T., Satoh, K., Saitoh, H., and Mishima, Y. (2005) The 3111T/C polymorphism of hClock is associated with evening preference and delayed sleep timing in a Japanese population sample. Am J Med Genet B Neuropsychiatr Genet *133*, 101-104.

Mohawk, J., Green, C., and Takahashi, J. (2012) Central and Peripheral Circadian Clocks in Mammals. Annu Rev Neurosci *35*, 445-462.

Nader, N., Chrousos, G.P., and Kino, T. (2009) Circadian rhythm transcription factor CLOCK regulates the transcriptional activity of the glucocorticoid receptor by acetylating its hinge region lysine cluster: potential physiological implications. FASEB J *23*, 1572-1583.

Niijima, A., Nagai, K., Nagai, N., and Nakagawa, H. (1992) Light enhances sympathetic and suppresses vagal outflows and lesions including the suprachiasmatic nucleus eliminate these changes in rats. J Auton Nerv Syst *40*, 155-160.

Numano, R., Yamazaki, S., Umeda, N., Samura, T., Sujino, M., Takahashi, R., Ueda, M., Mori, A., Yamada, K., and Sakaki, Y. (2006) Constitutive expression of the Period1 gene impairs behavioral and molecular circadian rhythms. Proc Natl Acad Sci U S A *103*, 3716-3721.

Park, N., Cheon, S., Son, G.H., Cho, S., and Kim, K. (2011) Chronic circadian disturbance by a shortened light-dark cycle increases mortality. Neurobiol Aging *33*, 1122.e1111-1122.

Pendergast, J.S., Friday, R.C., and Yamazaki, S. (2010) Photic entrainment of period mutant mice is predicted from their phase response curves. J Neurosci *30*, 12179-12184.

Popoli, M., Yan, Z., McEwen, B.S., and Sanacora, G. (2011) The stressed

synapse: the impact of stress and glucocorticoids on glutamate transmission. Nat Rev Neurosci *13*, 22-37.

Reddy, A.B., Maywood, E.S., Karp, N.A., King, V.M., Inoue, Y., Gonzalez, F.J., Lilley, K.S., Kyriacou, C.P., and Hastings, M.H. (2007) Glucocorticoid signaling synchronizes the liver circadian transcriptome. Hepatology *45*, 1478-1488.

Reddy, T.E., Gertz, J., Crawford, G.E., Garabedian, M.J., and Myers, R.M. (2012) The hypersensitive glucocorticoid response specifically regulates period 1 and expression of circadian genes. Mol Cell Biol *32*, 3756-3767.

Reddy, T.E., Pauli, F., Sprouse, R.O., Neff, N.F., Newberry, K.M., Garabedian, M.J., and Myers, R.M. (2009) Genomic determination of the glucocorticoid response reveals unexpected mechanisms of gene regulation. Genome Res *19*, 2163-2171.

Reppert, S.M., and Weaver, D.R. (2002) Coordination of circadian timing in mammals. Nature *418*, 935-941.

Revollo, J.R., and Cidlowski, J.A. (2009) Mechanisms generating diversity in glucocorticoid receptor signaling. Ann N Y Acad Sci *1179*, 167-178.

Robilliard, D.L., Archer, S.N., Arendt, J., Lockley, S.W., Hack, L.M., English, J., Leger, D., Smits, M.G., Williams, A., and Skene, D.J. (2002) The 3111 Clock gene polymorphism is not associated with sleep and circadian rhythmicity in phenotypically characterized human subjects. J Sleep Res

11, 305-312.

Sahar, S., and Sassone-Corsi, P. (2012) Regulation of metabolism: the circadian clock dictates the time. Trends Endocrinol Metab *23*, 1-8.

Scheer, F.A., Hilton, M.F., Mantzoros, C.S., and Shea, S.A. (2009) Adverse metabolic and cardiovascular consequences of circadian misalignment. Proc Natl Acad Sci U S A *106*, 4453-4458.

Schmutz, I., Ripperger, J.A., Baeriswyl-Aebischer, S., and Albrecht, U. (2010) The mammalian clock component PERIOD2 coordinates circadian output by interaction with nuclear receptors. Genes Dev *24*, 345-357.

Scott, D.K., Strömstedt, P.E., Wang, J.C., and Granner, D.K. (1998) Further characterization of the glucocorticoid response unit in the phosphoenolpyruvate carboxykinase gene. The role of the glucocorticoid receptor-binding sites. Mol Endocrinol *12*, 482-491.

Segall, L.A., Milet, A., Tronche, F., and Amir, S. (2009) Brain glucocorticoid receptors are necessary for the rhythmic expression of the clock protein, PERIOD2, in the central extended amygdala in mice. Neurosci Lett *457*, 58-60.

Shim, H.S., Kim, H., Lee, J., Son, G.H., Cho, S., Oh, T.H., Kang, S.H., Seen, D.S., Lee, K.H., and Kim, K. (2007) Rapid activation of CLOCK by Ca^{2+}-dependent protein kinase C mediates resetting of the mammalian

circadian clock. EMBO Rep *8*, 366-371.

So, A.Y., Bernal, T.U., Pillsbury, M.L., Yamamoto, K.R., and Feldman, B.J. (2009) Glucocorticoid regulation of the circadian clock modulates glucose homeostasis. Proc Natl Acad Sci U S A *106*, 17582-17587.

So, A.Y., Chaivorapol, C., Bolton, E.C., Li, H., and Yamamoto, K.R. (2007) Determinants of cell-and gene-specific transcriptional regulation by the glucocorticoid receptor. PLoS Genet *3*, e94.

Son, G.H., Chung, S., Choe, H.K., Kim, H.D., Baik, S.M., Lee, H., Lee, H.W., Choi, S., Sun, W., and Kim, H. (2008) Adrenal peripheral clock controls the autonomous circadian rhythm of glucocorticoid by causing rhythmic steroid production. Proc Natl Acad Sci U S A *105*, 20970-20975.

Strömstedt, P., Poellinger, L., Gustafsson, J., and Carlstedt-Duke, J. (1991) The glucocorticoid receptor binds to a sequence overlapping the TATA box of the human osteocalcin promoter: a potential mechanism for negative regulation. Mol Cell Biol *11*, 3379-3383.

Stratmann, M., and Schibler, U. (2006) Properties, entrainment, and physiological functions of mammalian peripheral oscillators. J Biol Rhythms *21*, 494-506.

Tahira, K., Ueno, T., Fukuda, N., Aoyama, T., Tsunemi, A., Matsumoto, S., Nagura, C., Matsumoto, T., Soma, M., Shimba, S*., et al.* (2011) Obesity alters the expression profile of clock genes in peripheral blood

mononuclear cells. Arch Med Sci *7*, 933-940.

Takahashi, J.S., Hong, H.K., Ko, C.H., and McDearmon, E.L. (2008) The genetics of mammalian circadian order and disorder: implications for physiology and disease. Nat Rev Genet *9*, 764-775.

Takano, A., Uchiyama, M., Kajimura, N., Mishima, K., Inoue, Y., Kamei, Y., Kitajima, T., Shibui, K., Katoh, M., and Watanabe, T. (2004) A missense variation in human casein kinase I epsilon gene that induces functional alteration and shows an inverse association with circadian rhythm sleep disorders. Neuropsychopharmacology *29*, 1901-1909.

Tamai, T., Carr, A., and Whitmore, D. (2005) Zebrafish circadian clocks: cells that see light. Biochem Soc Trans *33*, 962-966.

Todaro, G.J., and Green, H. (1963a) Quantitative studies of the growth of mouse embryo cells in culture and their development into established lines. J Cell Biol *17*, 299-313.

Todaro, G.J., and Green, H. (1963b) Quantitative studies of the growth of mouse embryo cells in culture and their development into established lines. J Cell Biol *17*, 299-313.

Toh, K.L., Jones, C.R., He, Y., Eide, E.J., Hinz, W.A., Virshup, D.M., Ptácek, L.J., and Fu, Y.H. (2001) An hPer2 phosphorylation site mutation in familial advanced sleep phase syndrome. Science *291*, 1040-1043.

Torra, I.P., Tsibulsky, V., Delaunay, F., Saladin, R., Laudet, V., Fruchart, J.C.,

Kosykh, V., and Staels, B. (2000) Circadian and glucocorticoid regulation of Rev-erbα expression in liver. Endocrinol *141*, 3799-3806.

Travnickova-Bendova, Z., Cermakian, N., Reppert, S.M., and Sassone-Corsi, P. (2002) Bimodal regulation of mPeriod promoters by CREB-dependent signaling and CLOCK/BMAL1 activity. Proc Natl Acad Sci U S A *99*, 7728-7733.

Ueda, H.R., Hayashi, S., Chen, W., Sano, M., Machida, M., Shigeyoshi, Y., Iino, M., and Hashimoto, S. (2005) System-level identification of transcriptional circuits underlying mammalian circadian clocks. Nat Genet *37*, 187-192.

Uhlenhaut, N.H., Barish, G.D., Yu, R.T., Downes, M., Karunasiri, M., Liddle, C., Schwalie, P., Hübner, N., and Evans, R.M. (2012) Insights into negative regulation by the glucocorticoid receptor from genome-wide profiling of inflammatory cistromes. Mol Cell.

Ukai-Tadenuma, M., Kasukawa, T., and Ueda, H.R. (2008) Proof-by-synthesis of the transcriptional logic of mammalian circadian clocks. Nat Cell Biol *10*, 1154-1163.

Ukai-Tadenuma, M., Yamada, R.G., Xu, H., Ripperger, J.A., Liu, A.C., and Ueda, H.R. (2011) Delay in feedback repression by cryptochrome 1 is required for circadian clock function. Cell *144*, 268-281.

Vanselow, K., Vanselow, J.T., Westermark, P.O., Reischl, S., Maier, B.,

Korte, T., Herrmann, A., Herzel, H., Schlosser, A., and Kramer, A. (2006) Differential effects of PER2 phosphorylation: molecular basis for the human familial advanced sleep phase syndrome (FASPS). Genes Dev *20*, 2660-2672.

Vatine, G., Vallone, D., Appelbaum, L., Mracek, P., Ben-Moshe, Z., Lahiri, K., Gothilf, Y., and Foulkes, N.S. (2009) Light directs zebrafish period2 expression via conserved D and E boxes. PLoS Biol *7*, e1000223.

Vitaterna, M.H., Takahashi, J.S., and Turek, F.W. (2001) Overview of circadian rhythms. Alcohol Res Health *25*, 85-93.

Wakamatsu, H., Takahashi, S., Moriya, T., Inouye, S.T., Okamura, H., Akiyama, M., and Shibata, S. (2001) Additive effect of mPer1 and mPer2 antisense oligonucleotides on light-induced phase shift. Neuroreport *12*, 127-131.

Welsh, D.K., Takahashi, J.S., and Kay, S.A. (2010) Suprachiasmatic nucleus: cell autonomy and network properties. Annu Rev Physiol *72*, 551-577.

Yamajuku, D., Shibata, Y., Kitazawa, M., Katakura, T., Urata, H., Kojima, T., Nakata, O., and Hashimoto, S. (2010) Identification of functional clock-controlled elements involved in differential timing of Per1 and Per2 transcription. Nucleic Acids Res *38*, 7964-7973.

Yamamoto, T., Nakahata, Y., Tanaka, M., Yoshida, M., Soma, H., Shinohara,

K., Yasuda, A., Mamine, T., and Takumi, T. (2005a) Acute physical stress elevates mouse period1 mRNA expression in mouse peripheral tissues via a glucocorticoid-responsive element. J Biol Chem *280*, 42036-42043.

Yamamoto, Y., Yagita, K., and Okamura, H. (2005b) Role of cyclic mPer2 expression in the mammalian cellular clock. Mol Cell Biol *25*, 1912-1921.

Yang, S., Liu, A., Weidenhammer, A., Cooksey, R.C., McClain, D., Kim, M.K., Aguilera, G., Abel, E.D., and Chung, J.H. (2009) The role of mPer2 clock gene in glucocorticoid and feeding rhythms. Endocrinology *150*, 2153-2160.

Yannielli, P., McKinley Brewer, J., and Harrington, M. (2002) Is novel wheel inhibition of Per1 and Per2 expression linked to phase shift occurrence? Neuroscience *112*, 677-685.

Yoo, S.H., Ko, C.H., Lowrey, P.L., Buhr, E.D., Song, E., Chang, S., Yoo, O.J., Yamazaki, S., Lee, C., and Takahashi, J.S. (2005) A noncanonical E-box enhancer drives mouse Period2 circadian oscillations in vivo. Proc Natl Acad Sci U S A *102*, 2608-2613.

Yoo, S.H., Yamazaki, S., Lowrey, P.L., Shimomura, K., Ko, C.H., Buhr, E.D., Siepka, S.M., Hong, H.K., Oh, W.J., and Yoo, O.J. (2004) PERIOD2:: LUCIFERASE real-time reporting of circadian dynamics reveals persistent circadian oscillations in mouse peripheral tissues. Proc Natl Acad Sci U S A *101*, 5339-5346.

Zheng, B., Larkin, D.W., Albrecht, U., Sun, Z.S., Sage, M., Eichele, G., Lee, C.C., and Bradley, A. (1999) The mPer2 gene encodes a functional component of the mammalian circadian clock. Nature *400*, 169-173.

Zylka, M.J., Shearman, L.P., Weaver, D.R., and Reppert, S.M. (1998) Three period Homologs in Mammals: Differential Light Responses in the Suprachiasmatic Circadian Clock and Oscillating Transcripts Outside of Brain. Neuron *20*, 1103-1110.

국문초록

글루코코르티코이드와 일주기시계 유전자의 분자적 상호작용

천솔미

일주기시계는 생명체의 생리 및 행동을 약 24시간의 주기로 조절해 주는 내재적인 생물학적 시계이다. 포유류의 일주기시계는 계층구조를 이루는데, 중추시계가 말초시계를 조절하는 것으로 알려져 있다. 중추시계는 뇌의 시상하부에 있는 시신경교차상핵으로, 신경 혹은 체액성 인자들을 통해 말초시계를 동기화한다. 동기화 인자들 중 가장 중요한 호르몬은 글루코코르티코이드 (glucocorticoid, GC) 인데, 이는 호르몬의 분비가 일주기리듬을 가지고 있으며, 중추시계를 제외한 거의 모든 세포에 도달하여, 일주기시계를 조절할 수 있는 능력을 가지고 있기 때문이다.

GC는 Period1 (Per1)과 Period2 (Per2)와 같은 일주기 시계 유전자를 직접 조절한다. 이 중 Per1의 프로모터 상에는 GC 반응서열 (GRE)가

잘 밝혀져 있었으나, Per2의 프로모터 상에서는 GRE가 알려져 있지 않았다. 본 연구에서는 GC가 다른 동기화 신호들에 비해 가장 강력하게 Per2의 발현을 유도하며, 일주기리듬의 위상이 늦어지게 하는 현상을 발견하였다. 또한, Per2 프로모터 상에서 GRE를 발견하였으며, 이 반응서열이 E-box와 1개의 염기서열이 겹쳐있는 것을 발견하였는데, 흥미롭게도 GRE 돌연변이 뿐만 아니라 E-box 돌연변이 또한 GC에 대한 반응성을 나타내지 못하였다, E-box 결합인자 중 하나인 Bmal1이 제거된 ($Bmal1^{-/-}$) 세포주에서 역시 GC에 의한 Per2의 발현 유도 현상이 감소하여, 일주기시계 인자인 Bmal1이 GC에 의한 Per2의 전사 활성을 일으키는 데에 필요하다는 것을 알게 되었다. Per1과 쥐 유선종양 바이러스 (mouse mammary tumor virus)와 같은 GRE를 포함하는 다른 유전자들의 프로모터는 $Bmal1^{-/-}$ 세포주에서도 GC에 대한 반응성이 감소하지 않는 것을 볼 때, Per2의 반응 기전은 독특한 것으로 생각되었다. 염색질 면역침강 (chromatin immunoprecipitation) 실험을 통해 알아본 결과, Bmal1은 Per2 프로모터의 GRE에 GC 수용체가 결합하는데 영향을 미치는 것으로 보인다. 또한, GRE에 의한 Per2 발현 조절의 중요성을 알기 위해, Per2 결함 ($Per2^{-/-}$) 세포주에 아데노바이러스를 이용하여 GRE 돌연변이를 도입한 Per2 프로모터를 통해 Per2가 발현되게 하여 세포주를 회복시키면, GC에 대한 Per2의 반응성이 감소하면서 일주기리듬의 위상이 앞당겨짐을 확인하였다. 따라서, 본 연구는 GC가 Bmal1과의 상호작용을

통해 Per2 프로모터의 GRE 활성을 조절하여 일주기리듬의 위상이 변화하는 것을 밝혀냄으로써, 일주기리듬의 조절기전을 밝혀내었다.

Per2와 같이 Bmal1에 의해 GC의 활성에 영향을 받는 유전자들이 많이 있을 것으로 생각되어, 추가로 마이크로어레이 실험을 수행하였다. 정상 세포주와 Bmal1$^{-/-}$ 세포주에 합성된 GC인 dexamethasone을 처리한 뒤, 마이크로어레이 실험을 수행한 결과를 이원분석법 (2-way ANOVA)을 통해 분석하였다. 그 결과, GC에 반응하는 유전자들 중, 절반 이상이 GC에 반응하는 데에 있어서 Bmal1에 영향을 받는 것을 알게 되었다. 이 유전자들이 특정 기능에 집중적으로 연관되어 있는지 생물정보 프로그램을 이용하여 분석해 본 결과, 외부자극에 대해 반응하는 유전자 및 당질화 및 산화·환원과 관련된 유전자들이 많이 포함되어 있었다. 즉, 본 연구에서는 유전체 전체적으로 GC의 작용기전에 Bmal1이 많은 영향을 미치고 있다는 것을 밝혀내었으며, 그 중에서도 외부 신호 전달, 당질화, 산화·환원 과정과 연관되어 있음을 알아내었다. 이는 앞으로 GC의 작용 기전에 대한 이해 및 GC와 생체시계와의 상호작용 연구에 많은 도움이 될 것으로 기대된다.

주요어: 일주기리듬(circadian clock), 글루코코르티코이드(glucocorticoid), Period2, Bmal1, 마이크로어레이

학 번: 2006-22971